A review of 3D printed concrete: performance requirements, testing measurements and mix design

Shaodan Hou[1], Jianzhuang Xiao* [1,2], Zhenhua Duan* [1,2], and Jun Ye[3]

[1] Department of Structural Engineering, Tongji University, Shanghai, PR China

[2] Key Laboratory of Performance Evolution and Control for Engineering Structures (Tongji University) Ministry of Education, PR China

[3] Department of Civil and Environmental Engineering, Imperial College London, London, UK.

*Corresponding author: Jianzhuang Xiao, E-mail: jzx@tongji.edu.cn, Tel: +86(021)-6598-2787; Zhenhua Duan, E-mail: zhduan@tongji.edu.cn.

Abstract: As one of the ways contributing to the progress of the industrialization of the construction industry, 3D printed concrete (3DPC) has attracted more and more attention in recent years. The utilization of 3DPC can accelerate the construction speed, save the labor and raw materials, as well as improve the design freedom of construction without formworks. However, one of the most significant challenges for the application of 3DPC is the ink materials. These is a big difference of the mixtures and performance between 3DPC and normal concrete. In order to provide an intensive reference for future studies to satisfy the performance requirements of 3DPC structures, this study firstly reviews the performance requirements of 3DPC, including the printability, fresh and hardened mechanical properties, and durability. Based on this, the specialized test methods for 3DPC are reviewed for the effective quality evaluation of 3DPC. The last part presents a review of mix design from the point of view of different materials and mix design approaches. The results show that 3DPC needs to meet the printability that it has higher requirements for rheology, hydration, and green strength than normal concrete. The interlayer bond is the key to study the anisotropic strength and durability degradation. More accurate test methods and testing standard should be developed. Besides, coarse aggregate and recycled materials need to be considered in the mix design of 3DPC.

Keywords: 3D printed concrete; printability; rheology; green strength; testing measurements; mix design

This is a peer-reviewed, accepted author manuscript of the following article: Hou, S., Duan, Z., Xiao, J., & Ye, J. (2021). A review of 3D printed concrete: performance requirements, testing measurements and mix design. Construction and Building Materials, 273, [121745]. https://doi.org/10.1016/j.conbuildmat.2020.121745

1 Introduction

As the progress of the industrialization of infrastructures, intelligent building technology has been increasingly applied in the built environment in recent years. Three-dimensional (3D) printing technology, as one form of intelligent buildings, is attracting more and more attention. According to an analysis of the publication output of 3D printing technology in the construction industry from 1997 to 2016, a quick increase trend was observed between 2013 and 2016 as shown in Fig. 1. The number of publications had almost doubled compared with that in 1997-2012, indicating that 3D printing technology is a research hotspot in the field of construction in the last few years [1]. Compared with the traditional construction methods, the application of 3D printing technology in the manufacturing of concrete structures has a high mechanization degree with fast construction speed and low labor consumption, which can lead to a lower cost. Besides, there are no formworks used with 3D printing technology in construction, resulting in a high degree of design liberalization and low resource consumption [2-7]. These advantages of 3D printing technology can resolve a series of problems facing traditional construction, including the low level of industrialization, severe environmental pollution, and the lacking of labor and excessive use of raw materials, etc.

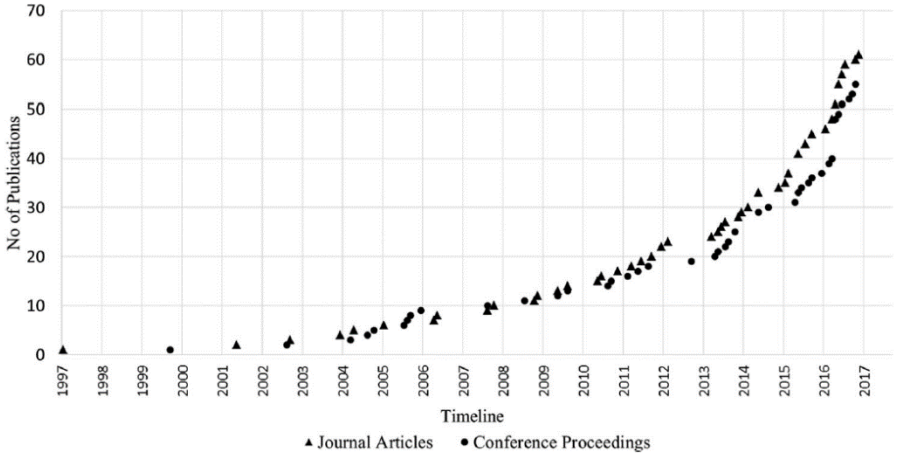

Fig.1 Trend of publication output from1997-2016 [1]

As the development of 3D printing technology, some buildings have already been printed in the world. In 2015, a 3D printed five-story apartment in China was constructed by WinSun company with the contour crafting technology [8]. The next year, Acciona Company using the D-shape technology to print a pedestrian bridge [9]. In 2019, a 3D printed bridge with a length of 26.3m was built by using the concrete printing technology in Shanghai [10]. Contour crafting and concrete printing [11,12] are the main construction mode for extrusion-based 3D printing technologies in construction industry currently. The materials for contour crafting and concrete printing are cementitious materials or geopolymer. Generally, mortar or paste with small aggregate particles is used in contour crafting. But concrete printing can apply concrete with coarse aggregate, which has potential to be applied in the large-scale structural prototypes. Thus, concrete printing is more suitable for the on-site construction, leading to more and more studies concentrating on concrete printing in recent years.

In order to fully understand the current development of 3D printing technology in construction industry, several reviews have been carried out [13-17]. The printing systems, materials, structural behavior, application, as well as cost and environment analysis of 3D printing technology in

construction industry were reviewed in these literatures. It can be concluded that the preparation of the main materials used for 3D printing technology, namely 3D printed concrete (3DPC), has become a significant challenge due to its great influence on the mechanical performance and printing process of printed structures. The special printability and anisotropic mechanical properties also put forward different requirements for the rheology, green strength, and interlayer bond of 3DPC compared with those of the normal concrete.

As a result, this study focuses on the review of concrete materials of 3DPC. Firstly, this study reviews the special performance requirements for 3DPC, including the printability (Section 2.1), fresh mechanical properties (Section 2.2), hardened mechanical properties (Section 2.2), and durability (Section 2.3). It helps the potential readers distinguish the requirements of 3DPC from that of normal concrete. Then a comparative analysis of some test methods on 3DPC is conducted to select some indexes that can effectively quantify its special requirements (Section 3), which is essentially necessary. Finally, the mix design of 3DPC is reviewed from the aspect of different materials and mix design approaches (Section 4). This study aims to provide a reference for future studies on 3DPC to develop new testing methods with effective evaluation indexes and optimize the mix proportions for better fresh and hardened properties.

2 Performance requirements of 3DPC

The preparation process of 3DPC generally includes mixing, delivery or pumping, extrusion, disposition and forming, and hardening. In this review study, the framework from extrusion to hardening are emphasized, as shown in Fig. 2. Due to the well-known characteristics of layer-by-layer construction without any formwork, the printability of fresh 3DPC, including extrudability and buildability that closely related to the rheological properties, and the fresh mechanical properties, are the key elements for its successful construction. In terms of the hardened properties of 3DPC, the mechanical and durability determine its service performance. The interlayer bond performance and anisotropy caused in the printing process are the research emphasis for the hardened properties of 3DPC.

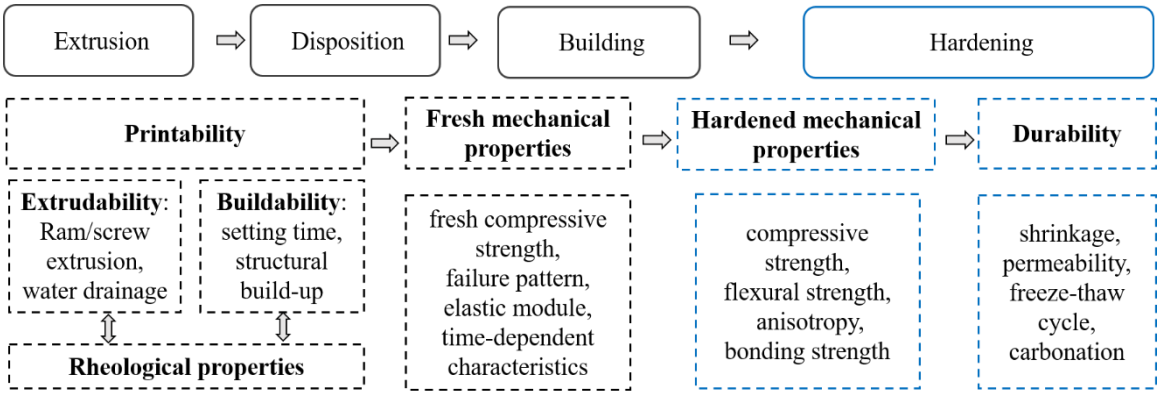

Fig. 2 The performance of 3DPC during the printing and hardened process

As a result, the review of this paper will be organized according to the above dataflow for the 3DPC framework, including printability, fresh and hardened mechanical properties, and then the printability, as shown in Fig.2. Detailed reviews will be presented in the following Sections.

However, due to the importance of testing measurement and mixed design on the properties of 3D printed concrete evaluation, reviews on these two aspects are also presented afterwards to better evaluate the performance for future research on 3DPC.

2.1 Printability

Printability, proposed as an important indicator to evaluate the behavior of fresh 3DPC, is related to the ability of the material/nozzle combination to produce a well-controlled filament [4]. However, its definition has not been completely unified. Buswell et al. [18] and Panda et al. [19] showed that printability can be evaluated by the deformation of the freshly printed components with certain layers, which was called buildability in other studies [20,21]. But Nerella et al. [22] defined it as a combination of delivery/pumping, extrudability, and buildability. As the theory of delivery/pumping for 3DPC can refer to that of normal concrete [23-26], the printability in this study is considered as the ability of fresh 3DPC to be extruded continuously and built up with acceptable deformation before setting, and it consists of extrudability and buildability, which will be explained in the following sections.

2.1.1 Extrudability

After mixing and delivery/pumping, the cementitious materials is fed into the hopper of extruder, from which the it is firstly pushed to the die and exit part and then extruded from the nozzle. Extrudability is defined as the ability to transport the fresh concrete to a nozzle in the hopper of the extruder as a continuous filament [27]. At present, screw extrusion and ram extrusion are the two most commonly used extrusion methods of 3DPC, their detailed comparison on the properties, requirements for flowable cementitious materials and application are shown in Table 1, and the working principle of the corresponding extruders is listed in Fig. 3. It is worth noting that the rheological behavior of cementitious materials has changed in the hopper of screw extruder (Fig. 3a) due to the existence of rotational screw, and the thixotropy of cementitious materials itself. In terms of ram extrusion (Fig. 3b), the cementitious materials are pushed by a ram inside the extruder barrel, with the shape of the extruded materials same to that of the extruder barrel. Compared with screw extrusion, the materials suitable for ram extrusion needs to have smaller fluidity and hardness. Besides, for traditional ram extrusion, a disadvantage that may hinder the industrial application of 3DPC is that cementitious materials can not be fed into the extruder continuously. Given this problem, Ji et al. [28] developed a double-assisted print head (Fig. 3c), which can continuously extrude the materials. Ram extrusion is generally used in the lab to evaluate the rheological properties and extrudability of materials [29-31], which will be discussed in Section 2.1.3.

During the extrusion process, 3DPC is required to be homogeneous and extruded continuously without any blockage, cracking and segregation [32]. Perrot et al. [33] conducted a review on the flow characteristics and rheological properties of extruded cement-based materials. They indicated that the pressing force to extrude materials is mainly composed of the forming force of the elongational flow and wall friction force of plug flow. The forming force is related to the rheological properties of elongational flow in the shaping zone, which can be calculated based on the Benbow and Bridgwater formula [34-36]. The wall friction force, occurred between materials and barrel surface, is influenced by the tribological behaviors of plug flow [30]. However, It is worth noting that the water drainage of 3DPC caused by extrusion will hinder its extrusion flow when it behaves inhomogeneous [37,38].

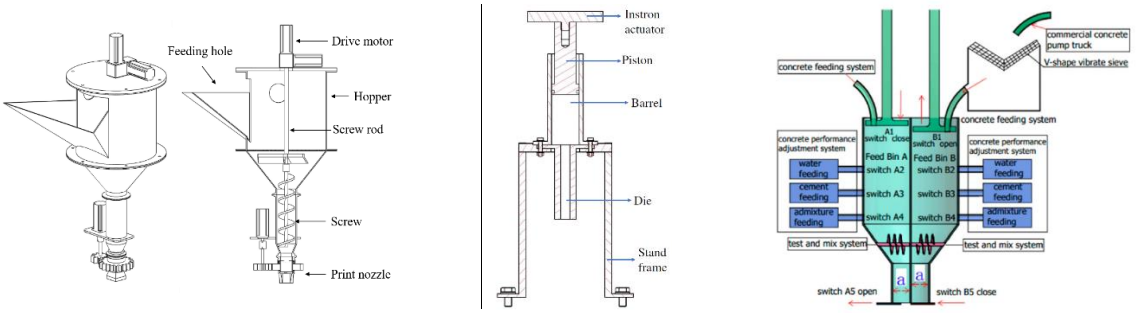

(a) screw extruder (b) ram extruder [39] (c) developed ram extruder [28]

Fig. 3 Working principle of different extruders

Table 1 A comparison of screw and ram extruder used for flowable 3DPC

	Properties	Requirements for cementitious materials	Applications
Screw extrusion (Fig. 3a)	➢ materials can be continuously fed into the extruder barrel ➢ the jamming of larger particles between the barrel of hopper and screw may occur	➢ homogeneous and high flowability ➢ high thixotropy ➢ accelerators are required for the short setting time	➢ Screw extrusion is more suitable for cement-based materials with fine aggregates, such as mortar
Ram extrusion (Figs. 3b and 3c)	➢ materials are sheared in the extruder ➢ materials can not be fed into the ram extruder continuously ➢ jamming problem may occur in the transition region from Barrel to Die	➢ greater viscosity is required to keep the shape after extruder ➢ lower flowability and higher yield stress	➢ Ram extrusion is suitable for concrete with large aggregates, such as concrete [28] ➢ ram extrusion can be used in the lab to evaluate the rheological properties and extrudability of material [29-31]

2.1.2 Buildability

Buildability is used to evaluate the ability of fresh 3DPC to bear its own weight, as well as the load of concrete from above layers, without collapse during printing. On the one hand, the 3DPC must be able to maintain its shape deformation within the controlled range after extrusion. The layer thickness is generally set to be small (varied from 1mm to 10cm) to limit the initial gravity stress to control the deformation [40]. The shear stress caused by gravity must be lower than the yield stress of cementitious materials to maintain its shape. The single-layer deformation of printed materials immediately after extrusion can be predicted by the developed model in literature [41,42], which is helpful for the analysis of buildability.

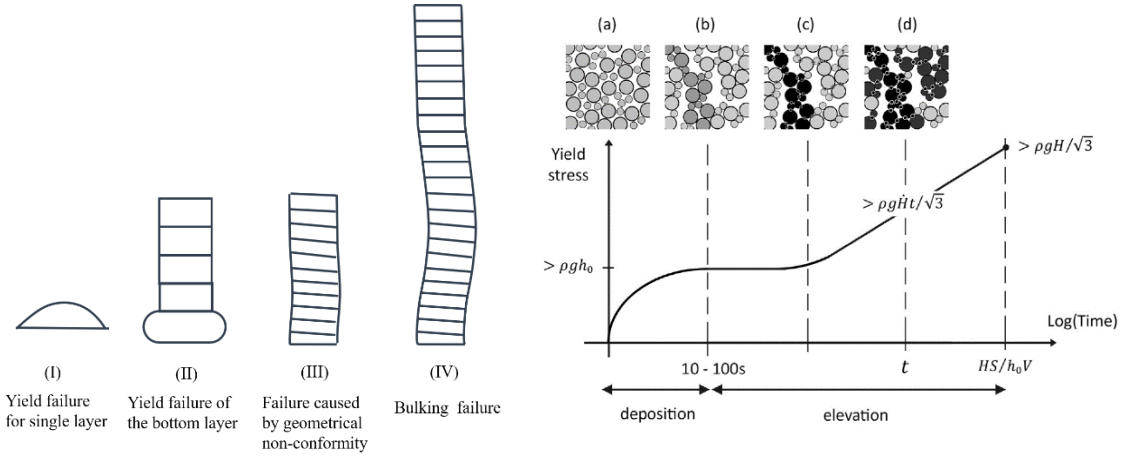

(a) different failure patterns (b) buildability analysis [40]

Fig. 4 Different failure patterns and buildability analysis of 3DPC

On the other hand, as the layers increase in the process of concrete printing, 3DPC elements are at a risk of collapse. Buildability, in this circumstance, also represents the ability of 3DPC elements to resist collapse stably at a specific height. According to the previous studies on the buildability of multi-layers 3DPC component, there are three failure modes for the layer-by-layer made component [40], as shown in Fig. 4a. Firstly, the stress from the upper layers increases as the layer number grows. There is a compressive failure risk in the bottom layer when the stress is higher than the yield stress. This failure mode depends on the comparison of the development of yield stress and the increase of stress as shown in Eq. (1) [43,46,47] while Fig. 4b shows the process of this failure mode. A lower bound analytical model was proposed to evaluate the buildability for plastic yielding of the bottom critical layer considering the stress redistribution of the printed layers in the printing process by Kruger et al. [48]. Secondly, the geometrical non-conformity that occurs in the printing process will lead to the collapse of the printing component. This is because of the accumulation of layer deformation, which is related to the evolution of elastic shear modulus and the rising speed of layers. Rigid materials with a fast growth of elastic modulus evolution are recommended for 3DPC. Thirdly, the bulking is dominant of failure when the printing component is a slender structure. It can be expected that compressive failure occurs when the number of layers is small while the bulking failure occurs when the number of layers increases. Based on the analysis, the critical height H_T between the two failure-criteria is shown in Eq. (2) [40]. In summary, the behavior of materials before the final setting needs to be studied and developed to enhance the buildability of 3DPC. Furthermore, the optimization of the printing system must be carried out since the properties of the printing process, such as open time[14], layer cycle time [6], etc., play an important role in the buildability.

$$\tau(t) > \rho g H / \sqrt{3} \quad (1)$$

$$H_T = 2\delta \sqrt{\frac{1+\nu}{3\sqrt{3}\gamma_c}} \quad (2)$$

where, τ is static yield stress, ρ is the density of 3DPC, H is the height of printing element, which depends on the rising speed and time, further, the rising speed is related to the speed of nozzle (H), the contour length scale (s) and thickness of layers (h_0) [40], δ is the width of the layer, ν is the Poisson coefficient, γ_c is the critical shear strain at flow onset.

2.1.3 Relationship between printability and rheology

From the above discussion, it is necessary to study the fresh properties of 3DPC to reveal its evolution mechanism and to further optimize its printability. Rheology, which can describe the evolution of viscosity, plasticity and elasticity of materials under shear stress, is applied in fresh concrete because cementitious materials behave as visco - plastic materials and exhibit non - Newtonian behavior [49].

In the process of screw extrusion, the cement-based material is sheared in the barrel. The material flows when the shear stress is higher than the corresponding dynamic yield stress. The rheological properties of materials have influenced the power of screw extrusion. For example, the greater screw power is required to maintain the same screw rotating speed for the materials with larger viscosity. Because the materials are sheared during the process of screw extrusion, the printable materials become more fluid at first, but then get stiffer with time. This can be explained by the thixotropy properties of printable materials. The rheological properties of printable materials after extrusion relate to the properties of the screw, including the rotate speed, shape, and the screw time. Nerella et al. [22,50] showed that there was a non-linear relationship between flow rate and rotational velocity because of the slippage at the elastomeric stator surface. In terms of ram extrusion, the flow of cementitious materials in the barrel is the same as that in pumping. A large part of the materials is un-sheared, and the shear occurs in a narrow zone between barrel wall and cementitious materials, called lubrication layer, at which the rheological properties (yield stress and plastic viscosity) of paste with fine particles determine the flow behavior of the cementitious materials. The cementitious materials are forming from the barrel zone to die zone, where the diameter of the barrel decreases, called the shaping zone. The forming force from the shaping zone is related to the rheological properties (yield stress) of the cementitious materials, as shown in Eq. 3 [30,34,35].

$$F_{\mathrm{pl}} = \frac{\pi D^2}{2}(\sigma_0 + \alpha V^{n_{BB}})\ln(\frac{D}{d}) \qquad (3)$$

where, F_{pl} is the forming force, σ_0 is the elongational yield stress, $\sigma_0 = \sqrt{3}\tau_0$, τ_0 is the yield stress of materials, α and n_{BB} are fitting parameters, D and d are the diameter of the barrel and die zone, respectively.

The extruded layer is basically at rest, and becomes stronger and more rigid with the layer by layer printing, which means that the static yield stress and shear elastic modulus are increasing. The static yield stress is the critical stress at a very low shear rate that the concrete begins to flow, and it is related to the thixotropic behavior of fresh concrete. It determines the ability of the printed layer to maintain shape after extrusion as shown in Eq. (1). When the concrete is at rest below the static yield stress, it exhibits the elastic behavior with the shear elastic modulus: $G = \tau_c/\gamma_c$, where τ_c is the static yield stress and γ_c is the critical shear strain [40]. The development of fresh 3DPC is mostly related to the increase of static yield stress and shear elastic modulus with time at rest, which can be attributed to the flocculation and hydration of binders. The parameter "structuration rate" was developed to predict the increase of static yield stress of cementitious material with time. Roussel et al. [51,52] developed a linear model to predict the structuration rate by testing the static yield stress at different rest time. It is worth noting that the structuration rate might no longer be constant and the relationship between static yield stress and time no longer be linear, because the 3DPC had more complex properties due to the addition of a higher amount of admixtures [53-57].

Nowadays, the research on the cementitious materials used in 3DPC is still at an early stage with many challenges. There are two important reasons for this. Firstly, the common test methods for fresh properties of normal concrete can not accurately capture the properties of 3DPC. On the other hand, the newly proposed evaluation methods are limited and a lack of sufficient experimental verification. At this circumstance, the rheology is a better choice for 3DPC with accurate results to describe the printability.

2.2 Mechanical properties

Mechanical properties of 3DPC are also very important, since they determine the practical application of 3DPC in construction directly. Compared with the normal concrete, the evolution of mechanical properties before final setting, the weak interface bond between layers, and the anisotropic mechanical properties are worth more attention.

2.2.1 Mechanical properties of fresh 3DPC

The development of mechanical properties of early age concrete from the plastic and deforming state to hardened state is very important for the 3D printing construction application. The early age mechanical properties have influenced the buildability, which further affects the construction process of 3DPC. Besides, the hardened properties are related to the fresh mechanical properties. It is reported that two clearly different stages of the development of the compressive strength and stress-strain relationship exist (as shown in Fig. 5a) [41,45,58]. Firstly, at the very young stage of the specimen forming process, there is a slow increase in green strength. The increase in strength is small but it will produce large deformations, and the stress-strain curve finally reaches a plateau condition. The failure mode of the specimen is barreling, similar to that of the plastic material, that the cross-sectional area increases as the vertical deformation increase. Secondly, as the development of hydration with time, the growth of compressive strength is faster. The increase of strength is growing until a peak value, after that the strength decreases, showing a brittle failure behavior of concrete. The lateral expansion is slight during this stage and a distinct failure plane can be found on the specimen. The layer-by-layer construction method requires rapid development of the compressive strength of 3DPC (as shown in Fig. 5b) to carry the stress from the above layers. By optimizing the mixtures of 3DPC, the demarcation of green strength to compressive strength varied from 30 min to 120 min in the previous studies [41,45,59]. The authors applied the recycled sand in 3DPC, leading to the fast development of early age strength, which can be attributed to the high water absorption of recycled sand [59]. In terms of the shear stress of 3DPC at the early age, it is shown that the variation trend of shear strength was similar to that of compressive strength with an equal development rate. The elastic modulus and cohesion increased linearly with ages while the Poisson's ratio and angle of internal friction remained constant [45].

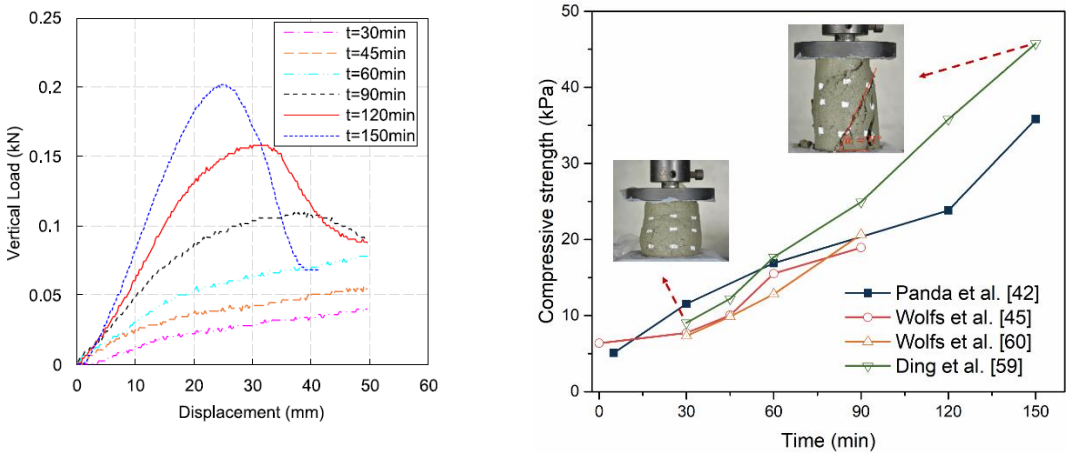

(a) Stress-displacement curve in early-ages [59]

(b) The development of compressive strength with time and cracking patterns of specimens

Fig. 5 The early age mechanical properties of extruded mortar

In order to predict the failure of 3DPC in the printing process, a model was proposed based on the first failure mode as described in Section 2.1.2 [45]. The green strength was found strongly related to the interparticle friction and cohesion, which could be evaluated based on the time-dependent Mohr-Coulomb failure criterion (Eq. 4). The time-dependent elastic modulus and Poisson's ratio were also applied in this model to estimate the stability of the printed element. The structural behavior was modelled by competing for the stepwise added layers and the development of mechanical behavior of materials with time during the printing process [45,60,61], that could be used to optimize the performance of fresh concrete.

$$\tau_y = C(t) + \sigma_n \cdot \tan(\varphi(t)) \quad (4)$$

where, τ_y is the shear yield stress, C is the cohesion, σ_n is the acting normal strength, φ is the angle of internal friction.

There is a risk of plastic cracking for the fresh 3DPC due to lack of curing, especially in severe environments, such as hot and windy conditions [62,63]. Moelich et al. [62] found that the cracks were formed in 2 hours after extrusion, which was earlier than that of normal concrete. Generally, the occurrence of plastic shrinkage is due to the rapid evaporation of water from the concrete surface, which results in certain shrinkage stress. Thus, the plastic cracks appear when the shrinkage stress is higher than the corresponding tensile stress, which is very low for fresh concrete. Fibers have been used in many research to improve the ductility of fresh 3DPC [64,65]. Besides, the printing process also influences the plastic crack. For example, the unmatched nozzle speed and extrusion speed will lead to the cracks. The high speed of nozzle will lead to tension stress on the filament when the extrusion speeds are kept the same, resulting in cracks on the surface of the concrete filament. The possibility of cracking increases in the outer edge with a small radius of the corner or wheel of the printing component [66].

2.2.2 Mechanical properties of hardened 3DPC

Compared with conventional concrete, the key problems of the mechanical properties of 3DPC are the interlayer bond strength and anisotropy. The reduced interlayer bond strength is not a new issue because the standard fluid concrete, such as self-compacting concrete, which also has a weak bond

strength, named “cold joint” or “distinct-layers casting” [6,67-69]. It is the weak interface bond that leads to the reduction of mechanical properties and durability of 3DPC [70-72]. The interlayer bond strength can be affected by a number of factors. Firstly, the parameters of the printing process, including the interval time, the print head speed, and the print nozzle height (Fig. 6), have great effects on the interface bond strength. As shown in Fig. 7a, the interface bond strength generally decreases with an increase of the interval time [27,71,73,74], since microstructure is denser with smaller voids and pores inside with a decreased time gap [75,76]. Panda et al. [77] developed the “time window” to evaluate the effect of interval time on the bond strength. The results showed that the effect was slight when the interval time was within the time window, otherwise, the effect was significant. Panda et al. [73,78] found that the low values of print head speed and the print nozzle standoff distance led to the increase of interface bond strength. While wolfs et al. [79] reported that there was no clear relation between nozzle height and interface bond strength.

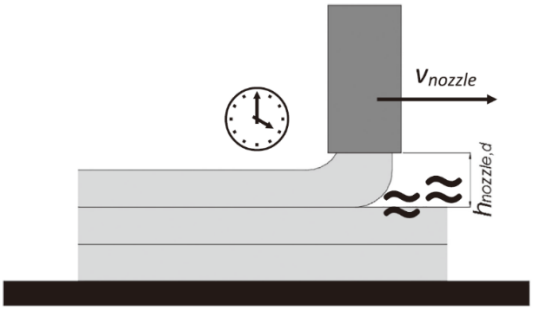

Fig. 6 The interface bond strength of 3DPC is related to several process parameters [4]

The properties of 3DPC also play a role in the interface bond strength. Roussel and Cussign [68] observed that the thixotropic property of cementitious materials had a negative effect on the interface bond strength, which was contradictory to the requirement of printability. Viktor et al. [80] found that the bond strength of 3DPC was related to the yield stress. The properties of 3DPC are affected by the properties of raw materials and mix proportions, and the detailed introduction will be discussed in section 4. The bond strength was further influenced by the printing environment and curing condition, which affected the surface moisture of samples and the activity of admixtures [81]. The high surface moisture content had a positive effect on the bond strength as shown in Fig. 7b [79,82].

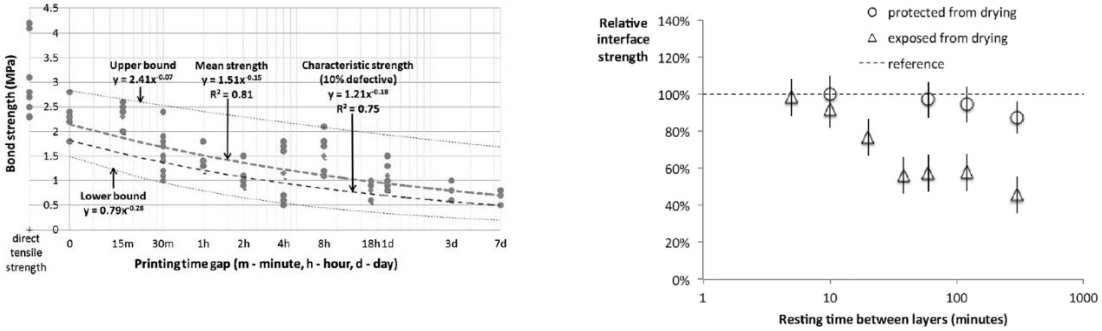

(a) Effect of printing time gap [71] (b) Effect of different drying conditions [40]

Fig. 7 Effect of printing time gap and surface moisture content on interface bond strength

A number of methodologies have been adopted to enhance the bond strength of 3DPC. Through adding a thin layer to glue the interlayers with paste [83,84] or polymer [85], a great enhancement

of bond strength can be achieved. Zareyian et al. [86] developed the effective interlocking on interlayer by adjusting the print nozzle opening geometry, showing an average increase of 26% on the bond strength. Therefore, various factors, including optimizing the printing process, properties of cementitious materials, and environmental conditions, need to be taken into account in 3D concrete printing to enhance its bond strength.

2.2.3 Influence of anisotropy on mechanical properties

The anisotropy of mechanical properties refers to the mechanical properties of 3DPC from different directions, which depend on inter-layer and inter-strip bonds [87]. The mechanical properties of 3DPC are influenced strongly by the printing direction. Le et al. [71] showed the minimum compressive strength occurred when the loading was parallel to the layers. Similar results of flexural strength were also found [65,87,88]. Table 2 shows the strength differences of 3DPC in different loading directions, which are evaluated by the standard deviation and variable coefficient. A significant range of standard deviation of compressive strength was obtained, which was because the different printing paths and fibers played a great role in the anisotropic mechanical properties of 3DPC [89,90]. The largest variation of compressive strength was obtained when the specimens were printed with fibers by the crosshatch shape [90]. Besides, the different printing paths might lead to cavities in concrete (Fig. 8a), which decrease the strength of 3DPC. A coefficient was defined by Ma et al. [64] to evaluate the anisotropic behaviors of mechanical properties of 3DPC (Eq. 5). The value of I_a was 0 for cast concrete, and the larger value (in the range of 0 to 1) of I_a indicated a greater anisotropy of material.

$$I_a = \sqrt{(f_x - f_c)^2 + (f_y - f_c)^2 + (f_z - f_c)^2} / f_c \qquad (5)$$

where, f_x, f_y *and* f_z are strength (contains compressive, flexural strength and so on) of 3DPC from three different directions, f_c is the strength of casted samples.

The anisotropic mechanical properties of 3DPC also leads to the difference between 3DPC and casted samples. Comparing the strength of printed specimens and casted specimens, both increase and decrease trend can be found (as shown in Table 2). The greatest reduction appears in the tension strength as expected.

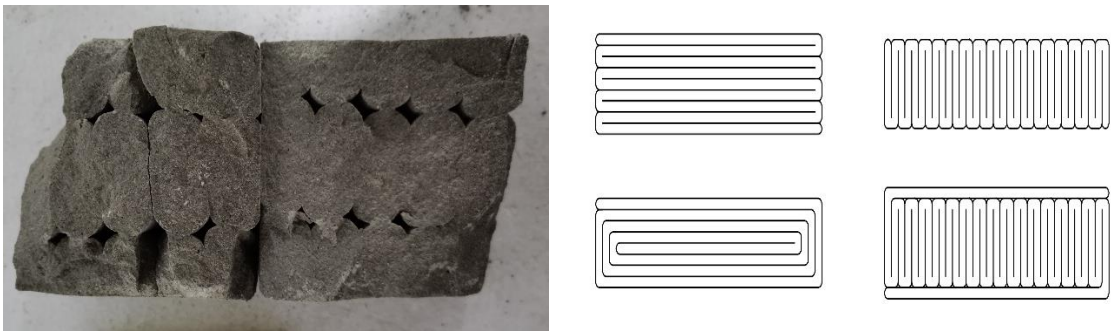

(a) The under-filling problem of 3DPC (b) Different printing paths for a printed beam

Fig. 8 The impact of printing paths on 3DPC performance

In conclusion, the key factor affects the anisotropy of strength is the weak interface bond strength, which leads to the degradation of mechanical properties and durability. The research on relationship

between the interface bond strength and the anisotropy of mechanical properties and durability, is still limited nowadays, and should be furtherly studied to improve the performance of 3DPC. In addition, the printing paths also have a great effect on the mechanical performance of 3DPC. Fig. 8b shows the common four different printing paths in one layer for a printed beam, different printing paths have a great effect on the structural behavior of 3DPC components as well as the thermal performance.

Table 2 The difference of strength of casted concrete and 3DPC with different loading direction (data from [64,65,71,79,87-91])

	Strength of 3DPC from different loading directions compared with casted samples	Variation of strength of 3DPC from different loading directions	
		standard deviation	variable coefficient
Compressive strength	67.4%-114.6%	0.53-**39.9**	2.4%-**70.8%**
Flexural strength	54.5%-157.1%	0.31-5.03	3.8%-43.1%
Tension strength	23.3%-112.2%	0.09-1.15	2.4%-11.9%
Elastic modulus	/	1.1-1.2	18.6%-43.7%

Note: The strength for casted samples were regarded as 1.

2.3 Durability

As the research of 3DPC is still in the primary stage, it mainly focuses on the mix design and early-age properties. Considering the importance of durability to the service life of concrete structure, the research on the durability of 3DPC, though still limited nowadays, needs to be emphasized. It is generally accepted that the durability of concrete depends on the concrete performance and the service environment. Some typical environmental factors that are adverse to the durability of concrete structures, include freeze-thaw cycle, carbonation, chloride penetration and alkali-aggregate reaction, most of which are related to the water transpiration process in the pores of concrete [92,93]. Therefore, the weak interface bond of 3DPC, caused by the loose microstructure with more and larger pores (as shown in Fig. 9), leads to the degradation of durability, and shall be considered in the future work. Moreover, the increase of cracks due to the shrinkage of 3DPC, which is the most concerned durability problem [6,94], will also lead to the decrease of its durability. The generation of greater plastic shrinkage and dry shrinkage can be attributed to the exposure of large area of the fresh printed concrete to the environment since no formwork is used in the printing process [71]. As there are already many effective solutions proposed to mitigate the shrinkage and crack of normal concrete, including internal curing, fibers, admixtures containing shrinkage-reducing and shrinkage-compensating and some other methodologies [95,96], their applicability to 3DPC should be carefully studied in the future.

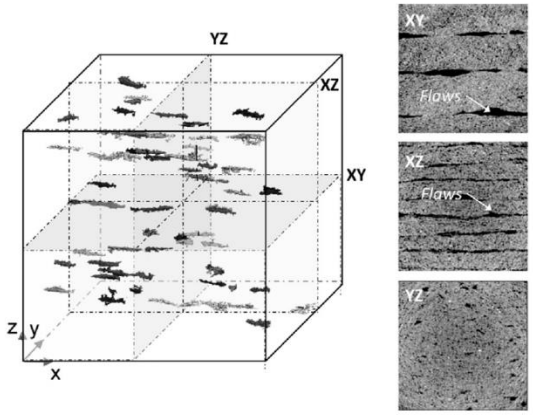

Fig. 9 The weak bond between interlayers of 3D printed concrete [64]

3 Testing measurements of 3DPC properties

In the review of the previous section, the property requirement of 3DPC is introduced in detail, on how they will affect the behavior of 3DPC. As a result, the methodologies to test and evaluate its properties is very important to better improve the property of 3DPC before they are widely used in practice. Available testing measurement methods of normal concrete and some newly developed testing methods are reviewed in this section. Different indexes are concluded and proposed to quantitatively evaluate the printability, mechanical properties, and durability of 3DPC.

3.1 Testing measurement of printability for 3DPC

Good printability is vital for the successful printing of 3DPC. Different from the workability of normal concrete, the printability required for 3DPC is more complex. Thus, most of the testing measurements for normal concrete are not suitable for use. However, the new developed parameters for evaluating the printability are limited in 3DPC. At this circumstance, rheological tests are applied in many studies, which can evaluate the printability with different rheological parameters. Therefore, the testing measurements from different studies for printability can be divided into three types in this study that will be summarized below.

3.1.1 Available conventional testing measurements

Although most of the conventional workability testing measurements for normal concrete are not regarded as the best testing measurements for 3DPC, some test methods, including slump and slump flow, are utilized with simple operation and low cost after determination of the suitable range for printing [20,97-100]. The slump and slump flow values with time were tested in the printing process until the 3D printing materials could not be successfully extruded or collapsing during the layer-by-layer building. The printable region was defined by the slump and slump flow values, which can be a preliminary reference for the mix design [99]. The slump and slump flow tests with time were also used to define the open time [27]. It should be noted that the printable region varied with the mixtures of 3DPC. Tay et al. [99] recommended the slump and slump flow of printable mortar in the range of 40-80 mm and 150-190mm, respectively. Ma et al. [20] advised a larger range of slump and slump flow of 32-88mm and 174-210mm. The variation of the printable region in

different studies is related to the characteristics of the printer head. The slump and slump flow values can be regarded as a preliminary reference to reflect the pintable region of 3DPC, but they cannot be able to accurately evaluate the printability. The conventional tests should be combined with some other methods to comprehensively evaluate the printable performance of 3DPC.

3.1.2 Newly developed testing measurements

The most intuitive test methods for printability are measuring the properties of components in the printing process as shown in Fig. 10. The extrudability can be evaluated by the shape of the printing specimens. The qualitative results of extrudability are defined as "YES" with continuous extrusion without blockage or fracture and "NO" with discontinued extrusion [27]. Besides, the deformation in the width of specimens determines the quality of the extrusion. The closer the specimen size is to the print nozzle size, the better is the extrudability (as shown in Fig. 10a). The variations of specimen shape and dimension, such as length, width, number and shape of filaments [20,27,98,101], are attracting attention from different studies because there is no standard for this test method at present. Besides, this method is conducted by visual observation with less accuracy, which is greatly affected by human factors and cannot be accurately and quantitatively used in the printing process.

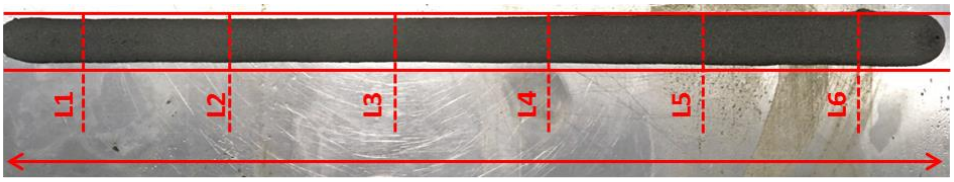

(a) The extrudability testing measurements

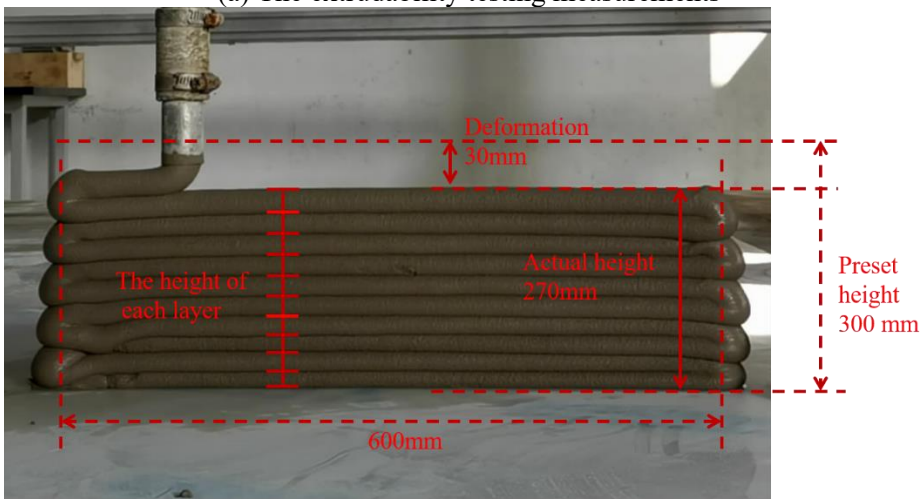

(b) The deformation of specimens to evaluate buildability

Fig. 10 Testing measurements during the printing process

In terms of the buildability, it was evaluated by the deformation of a certain layer [19-21,101,102] or the maximum layer without collapsing [27,97,100] in the printing process. Fig. 10b shows the deformation test for buildability. Low deformation and high maximum layers illustrate a better buildability. Similar problems also exist for extrudability where there is a measurement error in the testing process. Besides, the testing results are affected by the layer cycle time, printing speed, shape and size of each layer and machine precision. Generally, long cycle time, low printing speed

and high machine precision are beneficial to buildability. In terms of the printable element shape, the filament element has the minimum layer number compared with the rectangle or circle element when the material amount remains the same. The above-mentioned influencing factors lead to the difficulty of standardizing the test measurement. Although the testing measurements based on the printing process have some disadvantages, they are the most convenient methods with intuitive results at present. Therefore, more research should be conducted in the future to develop accurate and robust testing measurements during the printing process.

Nerella et al. [50] proposed an inline and quantitative method to characterize the extrudability of 3DPC with a new test device. The electric power consumption and extrudate flow rate were recorded at different rotational velocities of a progressive cavity pump. An index of unit extrusion energy (UEE), defined as the energy consumed per extruded unit volume, was developed to evaluate the extrudability. The lower the value of UEE, the higher the extrudability of 3DPC. For the current testing measurements, an adequate amount of materials needs to be extracted from the printing system, which leads to the waste of materials. Moreover, the tests are generally conducted after printing that they are unable to evaluate the test results effectively due to the time-dependent properties of fresh 3DPC. A real-time test method [97] was proposed through mounting a strain gage recording apparatus and wattmeter on the screw to record the real-time energy consumption of screw extruded motor. It can be used to evaluate the extrudability of 3DPC, and also to adjust the properties of 3DPC by adding admixtures during the printing process. Besides, the method can be used in a real scale application with real-time feedback and adjustments of fresh performance of 3DPC, which has great potential for application. In future research work, more attentions should be paid to the development of 3D concrete printing systems including the real-time testing of printability, feedback and adjusting. The evaluation parameters should not be only the energy consumption of the motor but also the rheological properties of fresh concrete for the comprehensive evaluation of the printability of 3DPC.

3.1.3 Rheology testing program

According to the previous discussion, it can be concluded that the research on the cementitious materials used in 3DPC is still in its infancy with many challenges. This is because the traditional parameters used for characterize the fresh properties of normal concrete are not suitable for accurate description of 3DPC. There is also a lack of newly developed evaluation indicators obtained from the printing process. Moreover, there is no standard for these testing measurements, which limited their widespread application. In this circumstance, rheology is a better choice for 3DPC with accurate results to describe the printability. Different testing programs were carried out to obtain the rheological parameters for 3DPC. The testing program includes the stepwise decreased rotational velocity/shear rate with each step getting an equilibrium stage, this is used to obtain the dynamic yield stress and plastic viscosity of 3DPC [100,103,104]. The torque vs. rotational velocity curves or shear rate vs. shear stress curves are obtained from this program. The Reiner-Riwlin equations (Eqs. 6-7) are used to transform the slope and intersection in the linear relationship of torque vs. rotational velocity curves to yield stress and plastic viscosity. The dynamic yield stress and plastic viscosity are obtained by fitting the curves with the Bingham model for a linear relationship or a Herschel model nonlinear relationship [105,106]. Also, the ram extruder is used as an appropriate tool to test rheological parameters of 3DPC as mentioned in Section 2.1.1 based on Eq. 3 [39,107]. The yield stress can be obtained by testing four different speeds with three varied dies with different sizes.

$$\tau_0 = \frac{\left(\frac{1}{R_1^2} - \frac{1}{R_2^2}\right)}{\ln\left(\frac{R_2}{R_1}\right) 4\pi h} \times G \quad (6)$$

$$\mu = \frac{\left(\frac{1}{R_1^2} - \frac{1}{R_2^2}\right)}{8\pi h^2} \times H \quad (7)$$

where, h is the height of vane, τ_0 is dynamic yield stress, μ is plastic viscosity, R_1 is the radius of vane, R_2 is the radius of the container, G is the intersection of the torque axis, H is the slope of the linear fitting curve of torque and speed.

Different testing programs were conducted to measure the thixotropic properties of 3DPC. In the first method, the thixotropy is evaluated by the area of hysteresis loop circled by the shear rate vs. shear stress curves [21,100]. The test protocol is shown in Fig. 11a. Generally, this method is difficult to quantitatively evaluate the thixotropic properties of 3DPC [52]. As regards the second testing program, it was developed to measure the flocculation properties of concrete to evaluate the structuration rate of concrete. The stress grow test is carried out to obtain the static yield stress by the maximum value at a very low speed (usually in the range of 0.001-0.1s^{-1}). Then the structuration rate (A_{thix}) was obtained by the evolution of static yield stress with time with the different developed models [19,78,98,102,108,109]. Sometimes, it is difficult to conduct the stress grow test for the stiffer 3DPC. In this case, a strain-based approach [110] was proposed to eliminate the limitation of the low shear rate. The constant shear strain was controlled when the shear rate varied from 0.08-0.24 s^{-1}. Thirdly, thixotropy index was evaluated by the relationship between the static and dynamic yield stress. Qian et al. [111] defined thixotropy index (I_{thix}) as $I_{thix} = \tau_i/\tau_e$, where τ_i and τ_e were the initial stress and equilibrium stress, respectively. In the study of Kolawole et al. [112] and Panda et al. [108], the thixotropy index = $(\tau_i-\tau_e/\ \tau_e)\times 100$. Fourthly, Panda et al. [102,108] developed a viscosity recovery test with 3 steps to simulate the different stages of the extruded materials, including the materials at rest before extrusion with a low shear rate for 60s, materials when extruding with a high shear rate for 30s and materials after extrusion with a low shear rate for 60s, to study the structural recovery behavior. The viscosity recovery degree was obtained by comparing the viscosity in the first and third steps (as shown in Fig. 11b). Materials with high viscosity recovery were suitable for 3DPC, showing the quick structural build-up properties.

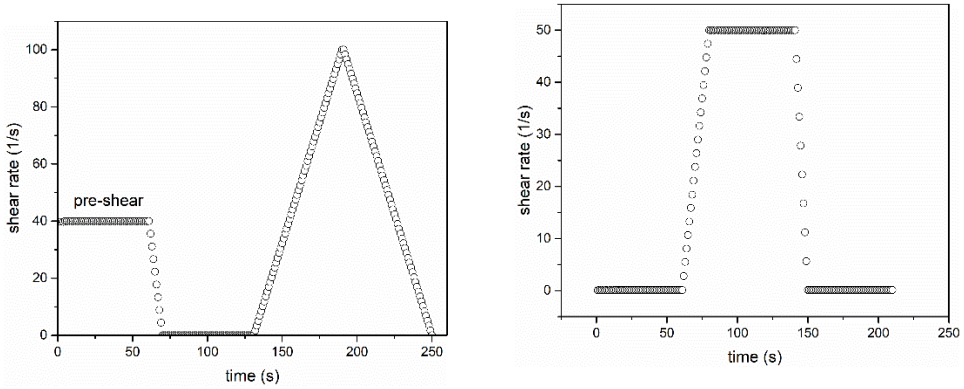

(a) Test protocol for hysteresis loop (b) Test protocol for viscosity recovery test

Fig. 11 Different test protocols for rheological tests

Although rheological tests were carried out in many previous studies for a comprehensive and accurate description of fresh 3DPC behavior, it is worth noting that the rheological results are easily disturbed by different factors, leading to erroneous conclusions [113]. Besides, the rheological tests are limited in measuring the 3DPC with high yield stress and viscosity.

3.2 Testing measurement of mechanical properties

The studies on mechanical properties of 3DPC includes the fresh mechanical properties, interlayer bonding strength and anisotropic mechanical properties in accordance to the difference of 3DPC and conventional concrete. Most of the testing measurements of the mechanical properties of 3DPC can be referred to previous studies on the soil and conventional concrete.

3.2.1 Testing measurement of mechanical properties of fresh 3DPC

The simplest test method to reflect the internal strengthening rate of 3DPC is the penetration test [103], which can be used at the very early age. The initial and final setting time obtained by the penetration test via the Vicat apparatus can evaluate the flocculation and hydration rate of materials, which further determines the stiffness development of 3DPC. Similarly, the hydration heat tests were used to help understand the internal strengthening performance of fresh 3DPC in literature [19,100,103].

Wolfs et al. [45] measured the fresh compressive strength by the unconfined uniaxial compression test according to geotechnical tests. The compressive strength, vertical and lateral deformation of specimens were recorded in the time range of 0-90 min after mixing and preparing. Each test was performed until the vertical strain reached 50%. Similar uniaxial compressive strength was used in literature [58,59,66]. At the same time, the direct shear test was conducted by two horizontal plates with a circular opening filled with compacting fresh concrete. Different loads were applied on the shear plate to get the parameters of C and φ in Eq. 4. Further, in order to simplify the tests, a triaxial compression test setup was developed to obtain all essential parameters from uniaxial compressive strength and direct shear strength tests based on the Mohr-Coulomb criterion [60]. The specimen was located in a closed chamber, where the air pressure was confining on the samples and the ram was used to apply pressure in the vertical direction of samples. Three different confining pressures were applied in the test at the age of 90 mins. The compressive strength, Young's modulus and Poisson's ratio were obtained when the confining pressure was 0. The cohesion and internal friction angle were obtained by the Mohr-Coulomb failure envelop as shown in Fig. 12(a).

It has been proved that the ultrasonic pulse velocity could be applied in testing the mechanical properties of hardened concrete [114,115]. In order to test the fresh mechanical properties for 3DPC with non-destructive methods, the ultrasonic pulse velocity was studied to test the fresh mechanical properties in literature [58,116]. Besides, the ultrasonic pulse velocity can be carried out continuously with less human error, which is appropriate for 3DPC. The linear relationship between ultrasonic pulse velocity waves by compression and elastic modulus or compressive strength was set up based on the testing results for 3DPC, as shown in Fig. 12(b), proving the feasibility of using ultrasonic pulse velocity to evaluate the fresh mechanical properties of 3DPC.

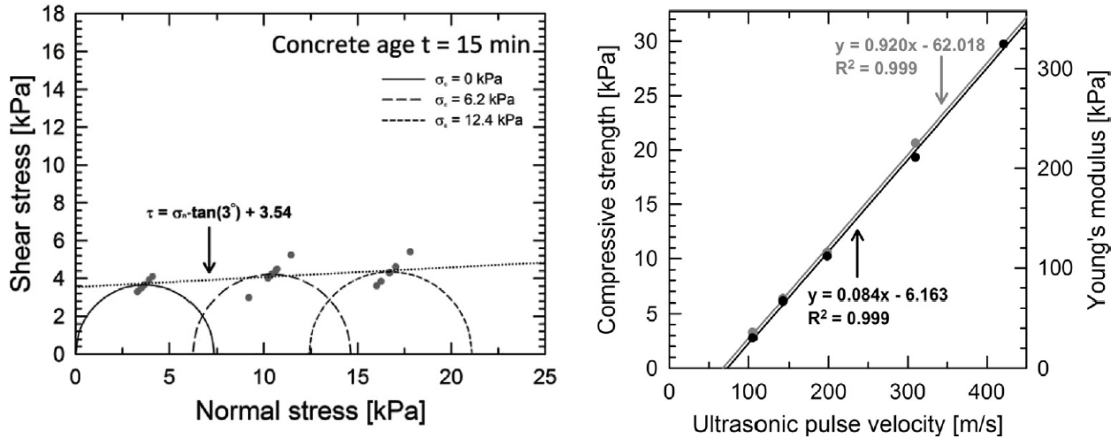

(a) Mohr-Coulomb failure envelopes for each concrete age as derived by TCT [60]

(b) Ultrasonic pulse velocity versus compressive strength (in black) and Young's modulus (in grey) [116]

Fig. 12 The analysis of results from different testing measurements for fresh strength of 3DPC

3.2.2 Testing measurement of mechanical properties for hardened 3DPC

The testing measurements for mechanical properties of hardened 3DPC, such as compressive and flexural strength, can be traced to those researches of measurements on conventional concrete. But the specimen preparation and the anisotropic test of 3DPC are still different from that of conventional concrete. With regard to the anisotropic test, it requires a different loading direction on the specimen, there are 3 loading directions for compressive strength and 2 loading directions for flexural strength [65,71,117], as shown in Fig. 13(a)-(b). The specimens for 3DPC are cut from the printed components and the size of which are sufficiently large. It should be noted that any interference during the cutting process, no matter a fresh state or hardened state of the component is in, may affect the accuracy of the test. Besides, there is a significant variation of the anisotropic strength considering the different printing paths. In terms of the interlayer bonding properties, Zareiyan et al. [86] reviewed different test methods as shown in Fig. 13(c), including the direct tensile test, splitting test, wedge splitting test, slant shear test, torsion bond test and shear strength test. The direct tensile test could be easily affected by the tension strength of the material and the results had great discreteness. The results of the splitting test were indirect tension. The results of the slant shear test were generally higher than other tests. At present, the most commonly used test methods for 3DPC are direct tensile test and splitting test [64,78]. Besides, the flexural strength could be used to evaluate the interlayer bond strength when the loading direction was the same as that in Fig. 13(d) [79,91]. This is because the flexural strength obtained in this direction is related to the interlayer bond properties.

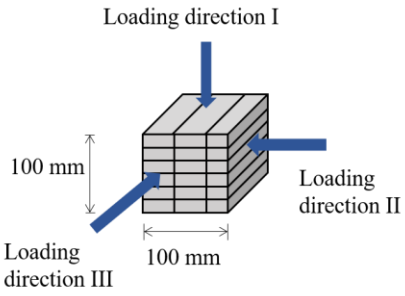

(a) Different loading direction for compressive strength of 3DPC

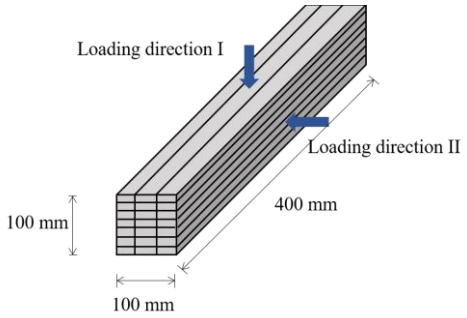

(b) Different loading direction for flexural strength of 3DPC

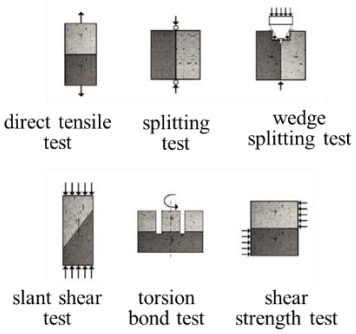

(c) Different test methods for interlayer bonding properties [86]

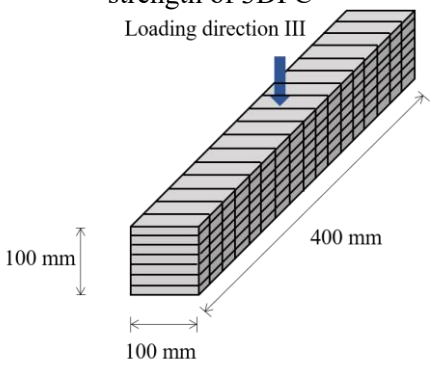

(d) The flexural strength to evaluate the interlayer bonding properties

Fig. 13 Test methods for anisotropic mechanical properties of 3DPC

Although the test methods for fresh and hardened strength of 3DPC according to the soil and conventional concrete have been carried out in many studies, there is no standard to normalize these test methods. For different studies, there are large differences in the loading speed, specimen size, preparing and curing of specimens, etc., making it difficult to compare their results directly. Therefore, it is of vital necessity to develop some universal standards for testing the printability and mechanical properties of 3DPC, and this is also beneficial to optimize the mixture and improve the properties of 3DPC, which will be discussed in Section 4. The test methods for the durability of conventional concrete will be applied to 3DPC in the future even though there is limited research on the durability of 3DPC nowadays. For example, the restrained shrinkage test and free shrinkage test were adopted to investigate the shrinkage of 3DPC [71,97,117]. Just as mentioned in Section 2.3, more tests on the microstructure should be conducted to study the durability evolution mechanism of 3DPC. Newly developed test methods are also necessary, such as the real-time testing of printability, ultrasonic pulse velocity measurement for fresh strength.

4 Mix design of 3DPC

4.1 Materials

The materials selected for the additive manufacturing process is an important part to meet the requirement of 3DPC. According to the high requirements of fresh properties of 3DPC, different supplement cementitious materials (SCMs), admixtures, fibers and aggregates are applied.

4.1.1 Supplement cementitious materials

The cement to aggregate ratio of 3DPC at present is much higher than that of normal concrete to achieve the required printability, which may lead to an increased cost. SCMs like fly ash, silica fume, limestone filler, and blast furnace slag, are used to partially replace cement. Table 3 shows the characteristic of different SCMs and their effects on the properties of concrete. Currently, there are already many studies [20,21,39,72,97,118,119] utilizing these SCMs as the materials of 3DPC.

As regards the research of different SCMs in 3DPC, Chen et al. [118] demonstrated that the combined use of silica fume and fly ash could be used to replace 45% of cement. Panda et al. [102] developed a type of 3DPC with a high volume of fly ash (45%-80% of binders by mass). Metakaolin was adopted to satisfy the buildability of 3DPC due to the improvement in thixotropy [120,121]. Nano silica, with an optimal dosage of 1%, was used to optimize the properties of 3DPC with increased re-flocculation rate, thixotropy and initial static yield stress[57,122]. The ternary binder system can enhance the fresh and hardened properties of concrete as well as reduce the CO_2 emissions [123], leading to sustainable 3DPC. Liu et al. [104] developed a mix design approach of 3DPC through a comparative study on the effect of individual and combined use of different cementitious materials on the rheological properties of concrete, and the optimal volume fraction for each component of different cementitious materials were also determined, in which the cement, fly ash and silica fume occupied 15%, 26% and 4% of the concrete volume, respectively. Nerella et al. [72] observed that 3DPC with binders of 55% cement, 30% fly ash and 15% micro silica had high strength and low anisotropy and less reduction of interface bond strength compared with cement 3DPC. The research by Papachristoforou et al. [97] indicated that the application of fly ash and ladle furnace slag to partly replace cement and limestone filler to partly replace sand had slight effect on the strength but significant positive effect on the durability of 3DPC.

Table 3 The SCMs used in concrete and their influence on concrete performance (results from literature [49,124-139])

	Characteristic	The influence of SCMs on rheological properties	The influence of SCMs on hardened properties
Fly ash	➢ high content of SiO_2 and Al_2O_3, low content of CaO, ➢ fine particle size in the range of 0.4-100μm, ➢ specific gravity in the range of 2.0-2.2, specific surface area varies from 300 to 500 m^2/kg, ➢ particle shape of class F fly ash is spherical with smooth surface.	➢ the addition of fly ash has a great effect on the rheological properties of concrete with different results, ➢ the varies in rheological properties are related to the type, particle size and particle shape of fly ash, ➢ class F fly ash has a greater effect on reducing the plastic viscosity than class C fly ash.	➢ low early strength and long setting time because of the lower early hydration heat of fly ash, ➢ the late-age mechanical properties and durability are enhanced by the secondary hydration effect of fly ash and $Ca(OH)_2$.
Silica fume	➢ high content of SiO_2, ➢ average particle size in the range of 0.1-0.3μm, ➢ specific surface area varies in the range of 20000-28000 m^2/kg.	➢ the addition of silica fume increases the yield stress, plastic viscosity and flocculation rate and decreases flowability of concrete, leading to the high uniformity and cohesiveness of concrete, ➢ the water to binder ratio and SP types has an important effect on the rheological properties of concrete with silica fume.	➢ the compressive and flexural strength are increased with the application of silica fume, ➢ there is a slight effect of silica fume on splitting strength, ➢ high content of silica fume increases the autogenous shrinkage.
Blast furnace slag	➢ high content of CaO, SiO_2 and Al_2O_3, ➢ specific gravity is about 2.9, ➢ specific surface area is in the range of 350-550 m^2/kg, ➢ bulk density varies from 1200 to 1300 kg/m^3.	➢ the addition of blast furnace slag can improve the workability and reduce the plastic viscosity, ➢ the yield stress of concrete is related to the replacement ratio and specific surface area of blast furnace slag.	➢ increasing the long-term compressive strength, enhancing the flexural strength, no matter early or later age, slight effects on the static elastic modulus, ➢ reducing the water and chloride ion permeability.
Limestone filler	➢ the main component is $CaCO_3$, ➢ particle size is from below 1 um to several tens of μm, ➢ irregular and rough particle shape, ➢ high adsorption ability of SP.	➢ in most cases, the addition of limestone filler increases the yield stress and plastic viscosity, ➢ the rheological properties of concrete depend on the specific surface area and particle size distribution of limestone filler.	➢ the addition of limestone filler may increase the compressive strength due to the filler effect and nucleation effect of the finer particles.
Metakaolin	➢ the main components are SiO_2 and Al_2O_3, ➢ a large part of the particles is smaller than 16um, the mean particle size is about 3μm, ➢ specific gravity is about 2.60, ➢ bulk density is in the range of 0.3-04 g/cm^3.	➢ the slump is reduced and the setting time is increased with the addition of metakaolin, ➢ increasing the thixotropy of concrete.	➢ increasing the compressive and flexural strength at a proper replacement ratio, ➢ reducing the ASR effects, shrinkage and permeability, which increase the durability.
Nano silica	➢ very high content of SiO_2, ➢ the average particle size is about 9 nm, the specific surface area is about 300 m^2/g.	➢ reducing the slump flow, slump and setting time, and increasing the yield stress and plastic viscosity due to the accelerating effect, ➢ the increase of yield stress is greater than plastic viscosity.	➢ refining the pore structure and leading to denser microstructure, ➢ enhancing the strength and durability of concrete due to its physical, acceleration and pozzolanic effects.

600

4.1.2 Admixtures

Different admixtures are necessary to improve the properties of 3DPC during different printing processes. Superplasticizer is almost applied in every mixture of 3DPC for the its capacity to successful extrusion. The addition of superplasticizer can reduce the yield stress and plastic viscosity of concrete due to the dispersion effect of the binder particles. It should be noted that the applied dosage of superplasticizer should be between the critical and saturation dosage.

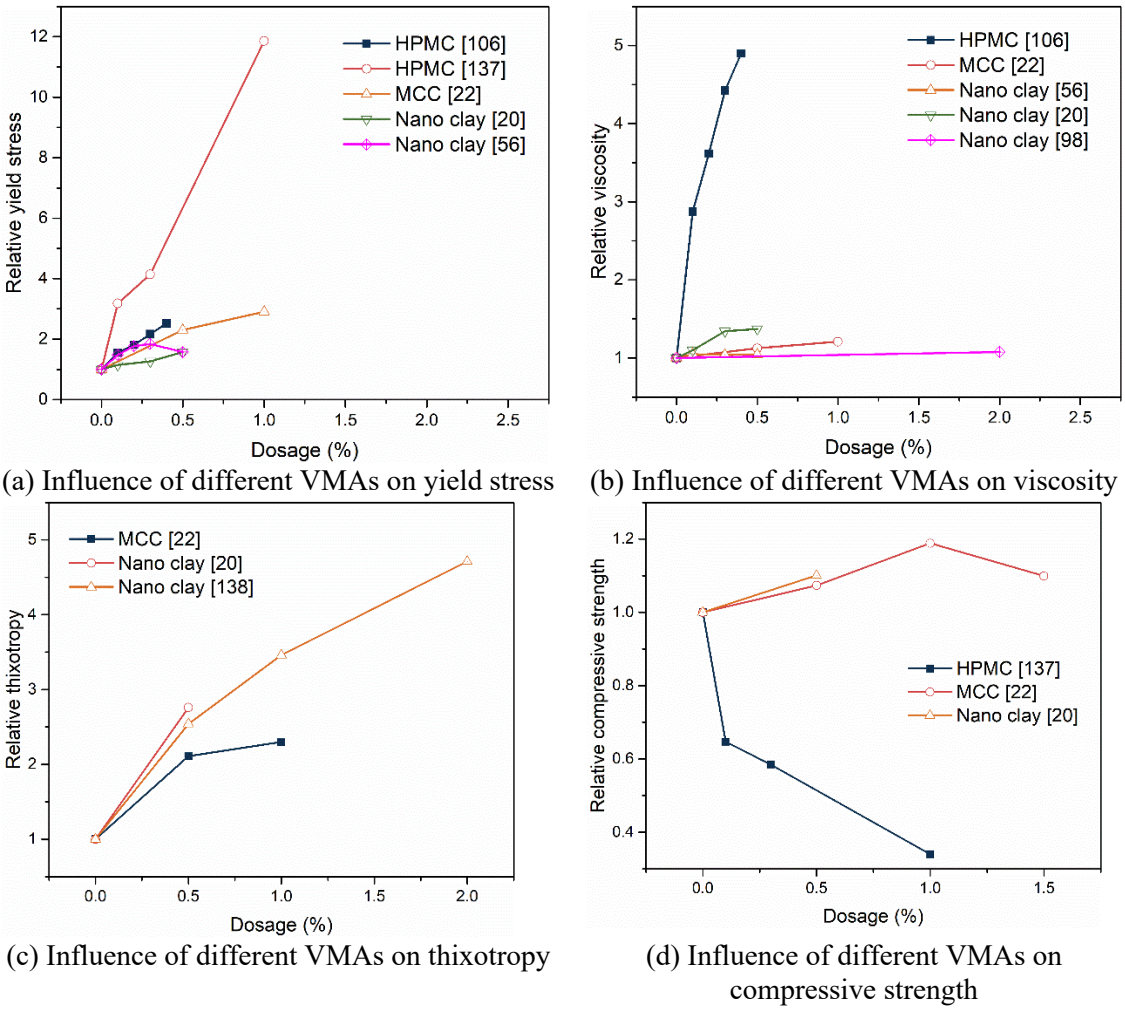

(a) Influence of different VMAs on yield stress

(b) Influence of different VMAs on viscosity

(c) Influence of different VMAs on thixotropy

(d) Influence of different VMAs on compressive strength

Fig. 14 Influence of different VMAs on the properties of 3DPC

Viscosity modified agent (VMA) was frequently used in 3DPC to enhance the viscosity and cohesion and then improve the shape stability after extrusion. The addition of VMA could increase the yield stress, viscosity and thixotropy with a shear-thinning behavior of cementitious materials [140]. The effect of VMA on concrete performance depended on the type and applied dosage. In terms of 3DPC, the most common types of VMA applied in the previous studies were cellulose-based VMA and nano clay. Fig. 14 shows the influence of different VMAs on the properties of 3DPC, where the data comes from different literatures as shown in Figs. 14 (a)-(d). The addition of hydroxy propyl methyl cellulose (HPMC) could remarkably enhance yield stress and viscosity, with the increase of extrusion pressure and shape retention of 3DPC [107]. However, as the dosage of HPMC increased, the 28-day compressive strength decreased greatly, which was caused by the delayed hydration degree of cement paste with HPMC and the increased air voids in concrete [141].

Both microcrystalline cellulose (MCC) [21] and nano clay increased the yield stress, viscosity, thixotropy and 28-day compressive strength of 3DPC. Nano clay, with a needle shape, was applied in the 3DPC because of its significant effect on the thixotropy [142-144]. A small amount of nano clay could remarkably enhance the thixotropy, further improve the buildability and green strength of 3DPC [19,56,100]. Rahul et al. [98] indicated that the combined use of silica fume, methyl cellulose-based VMA and nano clay could result in an appropriate mix design of 3DPC with improved robustness.

Accelerator and retarder were used to control the setting time of 3DPC. Accelerator, such as lithium carbonate [21], was recommended to obtain a short setting time to bear the stress from the upper layer. Retarder could delay the hydration process of cement, which were always used to control the setting time for concrete with high early strength cement [144]. The application of retarder could lead to a relatively smooth surface of the printable specimen. This is because the retarder, such as sodium gluconate, has the effect of reducing water and improve the fluidity of mortar at a suited dosage [145-147]. So, the free water increases in mortar, leading to the smooth surface of mortar. Although the addition of accelerator has been proved to be beneficial to the buildability and early strength, there are few studies applied it in the mixtures. This is because accelerator has a negative effect on the open time and extrudability, which may lead to the blockage of materials in the printing process. It is better to add the accelerator in the extruder nozzle or spray liquid accelerator on the printed element, which not only has a slight effect on the extrudability but also has a great effect on the structural build-up ability of concrete. The way of how to add accelerator is worthy of further study.

As discussed above, different types of SCMs and admixtures are used in 3DPC. Attentions should be paid to the interaction of different SCMs and admixtures to avoid poor performance. For example, the combined use of silica fume and polycarboxylate superplasticizer/sulfonated naphthalene polymer had a varied effect on the rheological properties of concrete [148]. The combined use of nano clay and polycarboxylate superplasticizer could lead to the high thixotropy and static yield stress of 3DPC with low dynamic yield stress [142].

4.1.3 Fibers

Considering the brittle failure modes of 3DPC, which are caused by the low ratio of tensile to compressive strength, reinforcement addition to the 3DPC is a good way to improve its structural property. However, embedding the reinforcement into the 3DPC continuously is difficult because of the layer-by-layer printing construction mode. Under this circumstance, the application of fibers attracted more attention. The organic fiber, steel fiber, basalt fiber, carbon fiber and glass fiber have been used in 3DPC. Organic fibers are the most commonly used including the polypropylene fiber, polyethylene fiber and polyvinylalcohol fiber. The addition of fiber had an evident impact on the flexural and tensile strength, which was caused by the alignment behavior of fiber after extrusion[65,90]. It should be noted that the increased flexural and tensile strength of 3DPC with fiber was dependent on the printing path [64]. However, the compressive strength and interface bond strength were only slightly increased but might be decreased by the addition of fiber. Panda et al. [65] found the glass fiber of 3mm could decrease the compressive strength because the fibers were parallel to the printing direction. Al-Qutaifi et al. [74] indicated that the steel fiber was not suitable for 3DPC because the protrusion of steel fibers could impede the adhesion of the interface layers. Generally, it is believed that a large volume of fibers had a negative effect on the extrudability and might cause the block in extrusion [31,64]. However, Ogura et al. [149] found that the volume of fiber was not the most important parameter to affect the extrusion. The increase in fibers could lead to a

decrease in the extrusion force. Soltan and Li [150] applied a typical fiber volume fraction for engineered cementitious composite (2% by volume) in 3D printing with improved tensile strain capacity and a high early age compressive strength. The steel cable, which is softer than the steel bar, has been adopted in 3DPC [89,151]. Lim et al. [151] embedded the steel cable into the extruded filament by a special device. In addition, the polyvinylalcohol fiber was hybrid adopted to prevent the cable slippage attributed to the interaction between the short fiber and microcracks caused by a long steel cable. The results showed that the hybrid reinforcement improved the flexural strength and the load for the first crack. The future study on applying fibers in 3DPC to improve the performance should concentrate on a number of directions. Firstly, a high volume of fiber can be used in 3DPC with good extrudability by optimizing the mixtures with different SCMs and admixtures. Secondly, the desired direction of fiber alignment can be obtained by adjusting the extrusion process. The future study on the optimal printing path with different fibers can be carried out.

4.1.4 Aggregates

Aggregates, which occupy a 60%-70% volume of concrete, play an important role in the performance of concrete. Compared with the cement paste, the yield stress and plastic viscosity are increased with the addition of aggregates, especially for aggregate with large gain size. Besides, the mechanical properties and shrinkage are related to the volume of aggregates. At present, only few studies applied coarse aggregates in 3DPC [28,101], most of the researchers studied 3D printed mortar without coarse aggregates. This is caused by the limitation of extrusion nozzle size and the complex properties of 3DPC with coarse aggregates. The volume friction and gradation greatly affect the rheological properties of 3DPC. Chaves Figueiredo et al. [39] found that the decrease of the maximum size of fine aggregate led to the development of the tight composite and increased the initial bulk yield stress. Zhang et al. [117] and Ogura et al. [149] found the sand to binder ratio had a great influence on the rheological properties and extrudability of 3DPC. The increase of sand to binder ratio led to the improvement of yield stress and plastic viscosity and the reduction of thixotropy.

As natural sandstone resources shortage, a series of policies and regulations to limit natural sand mining has been adopted in China, leading to the soaring prices of natural sand. At this circumstance, the sustainable aggregates were applied in 3DPC to replace sand. Ma et al. [20] used copper tailings to replace natural sand in 3DPC, they found that flowability increased and buildability decreased as the increase of the replacement ratio of copper tailings, which was caused by the finer particles of copper tailings. The best mixture was proposed with the replacement ratio of 40% of copper tailings with a sufficient buildability [152]. The research group of the authors investigated the feasibility of applying recycled sand and recycled powder to replace cement or natural sand in 3DPC [153-156]. A significant effect of recycled sand on the early age of mechanical behavior was obtained. The green strength and buildability were enhanced while the open time was reduced because of the high water absorption of recycled sand [59].

The application of coarse aggregates in 3DPC is an inevitable trend for a wide range of applications of 3DPC in construction. The tries have been carried out by Mechtcherine et al. [101] with a maximum aggregate size of 8 mm in 3DPC. A good extrudability in 90 mins and good buildability by printing 10 layers with a height of 500 mm in 30 min were proved. The mechanical properties of 3DPC with coarse aggregates in the largest loading direction were not significantly different from the casted specimen (in 10%). A large scale, on-site 3DPC building was introduced in literature [28]. The 3DPC with a maximum aggregate size of 15 mm was adopted. The slump of printed concrete was 110 mm and the initial setting was controlled in 5-10 mins by using

accelerators. The compressive strength of printed concrete was similar to a casted specimen. The study on the 3DPC with coarse aggregates is at the initial stage, which remains challenges for the application of coarse aggregates. The rheological properties are more complex with coarse aggregates, which are affected by the gradation and particle size, volume fraction of coarse aggregate, shape, and surface properties and so on. It also brings difficulties to test the rheological properties of 3DPC. This is because the present rheometers are used for high flowability concrete, which may have problems in testing stiffer 3DPC. Besides, the addition of coarse aggregates may increase the extrusion pressure, leading to the high requirement of the 3D printer.

4.2 3D printing geopolymer

Geopolymer is a sustainable construction material, which takes the by-products from industrial waste as raw materials. The application of geopolymer can reduce CO_2 emissions with high mechanical properties and good durability. The 3DPC made of geopolymer was developed with adequate printability and mechanical properties [74,89,157]. Generally, fly ash, silica fume and ground granulated blast-furnace slag were the most commonly used by-products in geopolymer. Panda et al. [108] used silica fume and ground granulated blast-furnace slag to enhance the properties of 3D printing fly ash-based geopolymer concrete. They found the ground granulated blast-furnace slag had a significant effect on the development of the structural build-up with a limited effect on the workability. The rheological properties of the geopolymer system were mostly affected by the addition of silica fume. The activator agent is another important component of geopolymer concrete, which can excite the activity of the by-products to be binding materials. The effect of Si/Na ratio of the activator on the performance of a 3D printing geopolymer was investigated. Zhang et al. [158] indicated that the Si/Na ratio of the activator affected the rheological properties of the geopolymer. The yield stress and structural rebuilding ability increased with the decrease of Si/Na ratio. Bong et al. [159] demonstrated that the Si/Na ratio significantly affected the open time and shape retention ability of 3D printing geopolymers. In terms of the influence of activator types, they found that the 3D printing geopolymer concrete with Na-based activators had higher compressive strength than that with K-based activators. The preparation process of geopolymer includes a conventional two-part mixing process. The alkaline solution is used in this process, which may bring difficulties in the extrusion process of 3D printing geopolymer concrete due to the higher viscosity of the alkaline solution. Besides, the waste alkaline solution is difficult to dispose of because of the corrosive properties. Under this circumstance, one-part geopolymers were used in 3DPC with a solid activator in literature [160,161]. The buildability was proved by printing a section with a height of 300 mm with slight deformation. The high viscosity recovery properties of 70%-80% in 60s demonstrated adequate extrudability. The results showed that a one-part geopolymer had the potential to be used in 3DPC with lower environmental impacts.

4.3 Mix design approaches for 3DPC

The mix design approaches need to satisfy the requirements of printability of 3DPC, which are related closely to the corresponding printer and printing process, making it different from the conventional concrete. In the mix design process of 3DPC, extrudability and buildability must be considered firstly to guarantee the successful printing process. Ma et al. [94] proposed a preparation procedure for the mix design of 3DPC according to the properties requirements of the printing process. The raw materials (cementitious materials and aggregates) were firstly determined based

on the requirement of extrudability considering the nozzle size. Then the admixtures, SCMs and fibers were added to satisfy the performance requirements of buildability, setting time, strength, and shrinkage of 3DPC. Besides, the inconsistent requirements of the concrete performance during different processes, such as the high flowability with high water to binder ratio for extrusion but low water to binder ratio for high strength, were balanced by the addition of superplasticizer. A similar opinion can be found in the literature [162], which indicated that the mixture for 3DPC must achieve the target goals of fresh properties. As we discussed before, the printability of 3DPC can be evaluated by the rheological properties. The studies on rheological properties revealed that the type and content of SCMs, the maximum aggregate size, the content of aggregate as well as admixtures have a significant effect on rheological properties of 3DPC [49,148]. Liu et al. [104] developed a mix design approach based on the correlation between SCMs (fly ash and silica fume) and rheological properties of printable materials. The multi-objectives optimization has been done based on the rheological requirements of printable materials to optimize the mix proportion. Le et al. [27] proposed an optimal mix by evaluating the extrudability and buildability through the workability of materials. Rahul et al. [98] presented a mix design approach based on yield stress. They found that the printable materials with the yield stress in the range of 1.5-2.5 kPa could meet the requirement of extrudability and buildability. Ivanova et al. [163] studied the effect of volume fraction and surface area of aggregate on the static yield stress of printable concrete. They found that the volume fraction had a more significant effect on static yield stress and buildability. The relationship between initial static yield stress and relative volume fraction was proposed, which contributed for the mix design of 3DPC. The Fuller and Thompson theory and the Marson-Percy model, which were usually used to optimize the gradation and packing fraction of sand for conventional concrete, were applied in designing the 3DPC by Weng et al. [164], and the effects of gradations on the rheological properties, related to the extrudability and buildability of 3DPC, were studied. The applicable 3DPC was developed by using the Fuller and Thompson theory and the Marson-Percy model, and it can be applied as a reference for 3DPC mixture design. Qian et al. [142] stated that the printability of 3DPC requires a balance of high static yield stress and low dynamic yield stress as well as the high thixotropy. They studied the compatibility of polycarboxylate superplasticizer and nano clay as well as the effect of these two materials on the rheological properties. The results showed that 0.2% of polycarboxylate superplasticizer and 0.5% of nano clay were benefit for the 3DPC. Different VMAs have been adopted in the mix design of 3DPC to meet the rheological requirements as we mentioned before.

Furthermore, Lu et al. [165] proposed a multi-level materials design including three inter-connected pyramids of mixture design, printing process and composite structure of 3DPC, as shown in Fig. 15. Two apexes were used to connected the three pyramids. The properties at the lower three apexes of each pyramid had a significant influence on the properties at the upper apex, which further affected the performance of the upper pyramid. The proposed multi-level materials design explained the contributions of each important factor on the performance of 3DPC, which gave a reference for future performance enhancement. Besides, the robustness of mixtures should be considered for mix design approaches. Rahul et al. [98] found that the addition of nano clay, VMA and silica fume could increase the robustness of mixtures.

As the development of high performance concrete, such as high fluidity concrete, self-compacting concrete, high strength concrete and so on, different mix design approaches have been proposed to obtain the high performance. Shi et al. [166] suggested 5 factors for designing the good mixtures for self-compacting concrete, which can be a reference for the mix design of 3DPC. They were (1) wide application, (2) strong robustness, (3) technical requirements, (4) sustainability and (5) cost.

Among them, the technical requirements are varied from different concrete, and the other 4 factors can apply to modern concrete, including 3DPC. Some mix design methods for self-compacting concrete can be used for 3DPC because the two types of concrete both have high requirements of rheological properties. Nowadays, since the development of 3DPC is at the initial stage, the studies on mix design approach for 3DPC are weak. More attentions should be paid on the mix design approaches of 3DPC in future for the better performance.

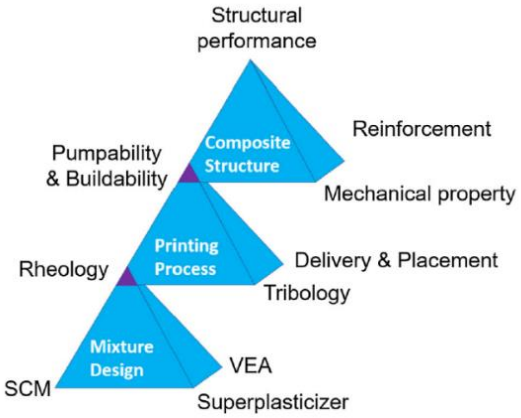

Fig. 15 The multi-level materials design from reference [165]

5 Conclusions and outlook

The development of 3D printing technology is beneficial for the construction industrialization and intelligent building. The greatest challenge of the application of 3D printing technology in construction is the materials-3D printed concrete (3DPC). Due to the layer-by-layer construction mode, the properties of 3DPC is different from normal concrete. Thus, the mix design for normal concrete is no more appropriate for 3DPC. It is necessary to review the performance requirements of 3DPC. Based on this, the testing measurement and evaluated indexes are reviewed. At last, the mix design of 3DPC is reviewed. The review can help to targeted evaluate and develop the properties of 3DPC, give some suggestions for the standardization of testing methods, and enhance the fresh and hardened properties of 3DPC. The following conclusions can be drawn:

- Performance requirement: The extrudability, buildability, open time and setting time are generally used to evaluate the fresh performance of 3DPC. Extrudability and buildability are related closely to the rheological properties, including the yield stress, viscosity and thixotropy. The evolution process of fresh mechanical properties depends on the hydration process of concrete. The weak interlayer bonding strength of 3DPC leads to the anisotropy of mechanical properties, which may result in a degradation of durability.
- Testing measurement: Some conventional tests method and rheological tests with different procedures, can obtain the yield stress, viscosity, thixotropy and have been used for 3DPC. Newly developed tests for extrudability and buildability according to the printing process have been developed. The inline and real-time testing measurements combined with the printer head with testing, feedback and adjusting system are recommended for the future work. Fresh mechanical properties tests can be carried out to obtain related design parameters according to the test methods of soil. Bond strength and anisotropic strength of 3DPC can be tested in the future via the test methods developed for conventional concrete. Testing standards for printability and mechanical properties of 3DPC are necessary in the future.

833 ● Mix design: The effects of different materials, including the supplement cementitious materials,
834 admixtures, fibers, and aggregates on the performance of 3DPC have been reviewed, aiming to help
835 select the raw materials for 3DPC. The requirements of printability should be firstly considered in
836 the development of mix design approaches. Recycled sand can be applied in 3DPC to improve its
837 performance. The high water absorption of recycled sand can significantly enhance the green
838 strength and buildability of 3DPC.
839 ● Outlook: The 3DPC is facing challenges from the factors of materials, testing methods and
840 machines. The robustness of 3DPC should be studied in the future to reduce the effect of the
841 variations of quality of raw materials, the printing conditions and so on. More SCMs and recycled
842 materials should be applied to reduce the CO_2 emission caused by the increased costs of 3D printing.
843 The mix design needs to be developed based on the printability. Durability is essential for the
844 service life of 3DPC. More reinforcement methods and printing strategies need to be developed for
845 a better structural behavior of 3DPC structures. The development of inline test methods with
846 feedback and conditioning system for fresh concrete in the printing process and the standard testing
847 measurements is necessary. Attention should be paid to the balance between the performance of
848 3DPC and printing characteristics, such as printing velocity and printer nozzle size. The 3D printer
849 with a large size of nozzle is required for printable concrete with coarse aggregates. Besides, the
850 large scale, onsite printer is suggested for the application of 3DPC in construction.
851

852 ## Acknowledgment

853 The financial support from the Jiangsu Renqiang Building Technology Company and the National
854 Natural Science Foundation of China (No: 51325802, 51708419, 51808399) are acknowledged.
855

856 ## References

857
858 [1] Tay YWD, Panda B, Paul SC, Noor Mohamed NA, Tan MJ, Leong KF. 3D printing trends in building
859 and construction industry: a review, Virtual and Physical Prototyping. 12(3) (2017) 261-76.
860 [2] Bhardwaj A, Jones SZ, Kalantar N, Pei Z, Vickers J, Wangler T, et al. Additive Manufacturing Processes
861 for Infrastructure Construction: A Review, J Manuf Sci E-T Asme. 141(0910109) (2019).
862 [3] Paolini A, Kollmannsberger S, Rank E. Additive manufacturing in construction: A review on processes,
863 applications, and digital planning methods, Additive Manufacturing. 30 (2019) 100894.
864 [4] Wangler T, Roussel N, Bos FP, Salet TAM, Flatt RJ. Digital Concrete: A Review, Cement Concrete Res.
865 123 (2019) 105780.
866 [5] Perkins I, Skitmore M. Three-dimensional printing in the construction industry: A review, International
867 Journal of Construction Management. 15(1) (2015) 1-9.
868 [6] Buswell RA, Leal De Silva WR, Jones SZ, Dirrenberger J. 3D printing using concrete extrusion: A
869 roadmap for research, Cement Concrete Res. 112 (2018) 37-49.
870 [7] Panda B, Tay YWD, Paul SC, Tan MJ. Current challenges and future potential of 3D concrete printing,
871 Materialwiss Werkst. 49(5) (2018) 666-73.
872 [8] http://www.winsun3d.com.
873 [9] https://www.autodesk.com/redshift/.
874 [10] https://www.archdaily.com/.
875 [11] Khoshnevis B. Automated construction by contour crafting — related robotics and information
876 technologies, Automat Constr. 13(1) (2004) 5-19.
877 [12] Shakor P, Sanjayan J, Nazari A, Nejadi S. Modified 3D printed powder to cement-based material and
878 mechanical properties of cement scaffold used in 3D printing, Constr Build Mater. 138 (2017) 398-409.
879 [13] Ma G, Wang L. A critical review of preparation design and workability measurement of concrete
880 material for largescale 3D printing, Front Struct Civ Eng. 12(3) (2018) 382-400.
881 [14] Siddika A, Mamun MAA, Ferdous W, Saha AK, Alyousef R. 3D-printed concrete: applications,
882 performance, and challenges, Journal of Sustainable Cement-Based Materials. (2019) 1-38.

[15] Zhang J, Wang J, Dong S, Yu X, Han B. A review of the current progress and application of 3D printed concrete, Composites Part A: Applied Science and Manufacturing. 125 (2019) 105533.
[16] Paul SC, van Zijl GPAG, Tan MJ, Gibson I. A review of 3D concrete printing systems and materials properties: current status and future research prospects, Rapid Prototyping J. 3(24) (2018) 784-98.
[17] Khan MA. Mix suitable for concrete 3D printing: A review, Materials Today: Proceedings. (2020).
[18] Buswell RA, Leal De Silva WR, Jones SZ, Dirrenberger J. 3D printing using concrete extrusion: A roadmap for research, Cement Concrete Res. 112 (2018) 37-49.
[19] Panda B, Ruan S, Unluer C, Tan MJ. Improving the 3D printability of high volume fly ash mixtures via the use of nano attapulgite clay, Composites Part B: Engineering. 165 (2019) 75-83.
[20] Ma G, Li Z, Wang L. Printable properties of cementitious material containing copper tailings for extrusion based 3D printing, Constr Build Mater. 162 (2018) 613-27.
[21] Long W, Tao J, Lin C, Gu Y, Mei L, Duan H, et al. Rheology and buildability of sustainable cement-based composites containing micro-crystalline cellulose for 3D-printing, J Clean Prod. 239 (2019) 118054.
[22] Nerella VN, Mechtcherine V. Chapter 16 - Studying the Printability of Fresh Concrete for Formwork-Free Concrete Onsite 3D Printing Technology (CONPrint3D). In: Editor, JG Sanjayan, A Nazari, B Nematollahieditors. 3D Concrete Printing Technology: Butterworth-Heinemann, 2019. 333-47.
[23] Jang KP, Choi MS. How affect the pipe length of pumping circuit on concrete pumping, Constr Build Mater. 208 (2019) 758-66.
[24] Secrieru E, Fataei S, Schröfl C, Mechtcherine V. Study on concrete pumpability combining different laboratory tools and linkage to rheology, Constr Build Mater. 144 (2017) 451-61.
[25] Secrieru E, Mohamed W, Fataei S, Mechtcherine V. Assessment and prediction of concrete flow and pumping pressure in pipeline, Cement and Concrete Composites. 107 (2020) 103495.
[26] Tichko S, Van De Maele J, Vanmassenhove N, De Schutter G, Vierendeels J, Verhoeven R, et al. Numerical simulation of formwork pressure while pumping self-compacting concrete bottom-up, Eng Struct. 70 (2014) 218-33.
[27] Le TT, Austin SA, Lim S, Buswell RA, Gibb AGF, Thorpe T. Mix design and fresh properties for high-performance printing concrete, Mater Struct. 45(8) (2012) 1221-32.
[28] Ji G, Ding T, Xiao J, Du S, Li J, Duan Z. A 3D Printed Ready-Mixed Concrete Power Distribution Substation: Materials and Construction Technology, Materials. 12(9) (2019) 1540.
[29] Alfani R. Rheological test methods for the characterization of extrudable cement-based materials - A review, Mater Struct. 38(276) (2005) 239-47.
[30] Perrot A, Mélinge Y, Rangeard D, Micaelli F, Estellé P, Lanos C. Use of ram extruder as a combined rheo-tribometer to study the behaviour of high yield stress fluids at low strain rate, Rheol Acta. 51(8) (2012) 743-54.
[31] Zhou X. Characterization of rheology of fresh fiber reinforced cementitious composites through ram extrusion, Mater Struct. 38(275) (2005) 17-24.
[32] El Cheikh K, Rémond S, Khalil N, Aouad G. Numerical and experimental studies of aggregate blocking in mortar extrusion, Constr Build Mater. 145 (2017) 452-63.
[33] Perrot A, Rangeard D, Nerella V, Mechtcherine V. Extrusion of cement-based materials - an overview, RILEM Technical Letters. 3 (2018) 91-7.
[34] Benbow JJ, Jazayeri SH, Bridgwater J. The flow of pastes through dies of complicated geometry, Powder Technol. 65(1) (1991) 393-401.
[35] Benbow JJ, Oxley EW, Bridgwater J. The extrusion mechanics of pastes—the influence of paste formulation on extrusion parameters, Chem Eng Sci. 42(9) (1987) 2151-62.
[36] Benbow JJ. The dependence of output rate on die shape during catalyst extrusion, Chem Eng Sci. 26(9) (1971) 1467-73.
[37] Martin PJ, Wilson DI, Bonnett PE. Paste extrusion through non-axisymmetric geometries: Insights gained by application of a liquid phase drainage criterion, Powder Technol. 168(2) (2006) 64-73.
[38] Khelifi H, Perrot A, Lecompte T, Rangeard D, Ausias G. Prediction of extrusion load and liquid phase filtration during ram extrusion of high solid volume fraction pastes, Powder Technol. 249 (2013) 258-68.
[39] Chaves Figueiredo S, Romero Rodríguez C, Ahmed ZY, Bos DH, Xu Y, Salet TM, et al. An approach to develop printable strain hardening cementitious composites, Mater Design. 169 (2019) 107651.
[40] Roussel N. Rheological requirements for printable concretes, Cement Concrete Res. 112 (2018) 76-85.
[41] Panda B, Lim JH, Tan MJ. Mechanical properties and deformation behaviour of early age concrete in the context of digital construction, Composites Part B: Engineering. 165 (2019) 563-71.

[42] Khoshnevis B, YUAN X, Zahiri B, Zhang J, Xia B. Deformation Analysis of Sulfur Concrete Structures Made by Contour Crafting. AIAA SPACE FORUM. Pasadena, Calofornia2015. 14.
[43] Perrot A, Rangeard D, Pierre A. Structural built-up of cement-based materials used for 3D-printing extrusion techniques, Mater Struct. 49(4) (2016) 1213-20.
[44] Reiter L, Wangler T, Roussel N, Flatt RJ. The role of early age structural build-up in digital fabrication with concrete, Cement Concrete Res. 112 (2018) 86-95.
[45] Wolfs RJM, Bos FP, Salet TAM. Early age mechanical behaviour of 3D printed concrete: Numerical modelling and experimental testing, Cement Concrete Res. 106 (2018) 103-16.
[46] Wangler T, Lloret E, Reiter L, Hack N, Gramazio F, Kohler M, et al. Digital Concrete: Opportunities and Challenges, RILEM Technical Letters. 1 (2016) 67-75.
[47] Roussel N, Coussot P. “Fifty-cent rheometer” for yield stress measurements: From slump to spreading flow, J Rheol. 49(3) (2005) 705-18.
[48] Kruger J, Zeranka S, van Zijl G. 3D concrete printing: A lower bound analytical model for buildability performance quantification, Automat Constr. 106 (2019) 102904.
[49] Jiao D, Shi C, Yuan Q, An X, Liu Y, Li H. Effect of constituents on rheological properties of fresh concrete-A review, Cement and Concrete Composites. 83 (2017) 146-59.
[50] Nerella VN, Näther M, Iqbal A, Butler M, Mechtcherine V. Inline quantification of extrudability of cementitious materials for digital construction, Cement and Concrete Composites. 95 (2019) 260-70.
[51] Roussel N, Ovarlez G, Garrault S, Brumaud C. The origins of thixotropy of fresh cement pastes, Cement Concrete Res. 42(1) (2012) 148-57.
[52] Roussel N. A thixotropy model for fresh fluid concretes: Theory, validation and applications, Cement Concrete Res. 36(10) (2006) 1797-806.
[53] Lecompte T, Perrot A. Non-linear modeling of yield stress increase due to SCC structural build-up at rest, Cement Concrete Res. 92 (2017) 92-7.
[54] Mettler LK, Wittel FK, Flatt RJ, Herrmann HJ. Evolution of strength and failure of SCC during early hydration, Cement Concrete Res. 89 (2016) 288-96.
[55] Weng Y, Lu B, Li M, Liu Z, Tan MJ, Qian S. Empirical models to predict rheological properties of fiber reinforced cementitious composites for 3D printing, Constr Build Mater. 189 (2018) 676-85.
[56] Ma S, Qian Y, Kawashima S. Experimental and modeling study on the non-linear structural build-up of fresh cement pastes incorporating viscosity modifying admixtures, Cement Concrete Res. 108 (2018) 1-9.
[57] Kruger J, Zeranka S, van Zijl G. An ab initio approach for thixotropy characterisation of (nanoparticle-infused) 3D printable concrete, Constr Build Mater. 224 (2019) 372-86.
[58] Voigt T, Malonn T, Shah SP. Green and early age compressive strength of extruded cement mortar monitored with compression tests and ultrasonic techniques, Cement Concrete Res. 36(5) (2006) 858-67.
[59] Ding T, Xiao J, Qin F, Duan Z. Mechanical behavior of 3D printed mortar with recycled sand at early ages, Constr Build Mater. 248 (2020) 118654.
[60] Wolfs RJM, Bos FP, Salet TAM. Triaxial compression testing on early age concrete for numerical analysis of 3D concrete printing, Cement and Concrete Composites. 104 (2019) 103344.
[61] Jayathilakage R, Rajeev P, Sanjayan JG. Yield stress criteria to assess the buildability of 3D concrete printing, Constr Build Mater. 240 (2020) 117989.
[62] Moelich GM, Kruger J, Combrinck R. Plastic shrinkage cracking in 3D printed concrete, Composites Part B: Engineering. 200 (2020) 108313.
[63] Makul N. Advanced smart concrete - A review of current progress, benefits and challenges, J Clean Prod. 274 (2020) 122899.
[64] Ma G, Li Z, Wang L, Wang F, Sanjayan J. Mechanical anisotropy of aligned fiber reinforced composite for extrusion-based 3D printing, Constr Build Mater. 202 (2019) 770-83.
[65] Panda B, Chandra Paul S, Jen Tan M. Anisotropic mechanical performance of 3D printed fiber reinforced sustainable construction material, Mater Lett. 209 (2017) 146-9.
[66] Bos F, Wolfs R, Ahmed Z, Salet T. Additive manufacturing of concrete in construction: potentials and challenges of 3D concrete printing, Virtual and Physical Prototyping. 11(3) (2016) 209-25.
[67] Assaad JJ. Correlating Thixotropy of Self-Consolidating Concrete to Stability, Formwork Pressure, and Multilayer Casting, J Mater Civil Eng. 28(0401610710) (2016).
[68] Roussel N, Cussigh F. Distinct-layer casting of SCC: The mechanical consequences of thixotropy, Cement Concrete Res. 38(5) (2008) 624-32.
[69] Wael AMAK. Bond Strength in Multilayer Casting of Self-Consolidating Concrete, Aci Mater J. 114(3) (2017).

994 [70] Nerella VN, Hempel S, Mechtcherine V. Effects of layer-interface properties on mechanical
995 performance of concrete elements produced by extrusion-based 3D-printing, Constr Build Mater. 205 (2019)
996 586-601.
997 [71] Le TT, Austin SA, Lim S, Buswell RA, Law R, Gibb AGF, et al. Hardened properties of high-
998 performance printing concrete, Cement Concrete Res. 42(3) (2012) 558-66.
999 [72] Nerella VN, Hempel S, Mechtcherine V. Effects of layer-interface properties on mechanical
1000 performance of concrete elements produced by extrusion-based 3D-printing, Constr Build Mater. 205 (2019)
1001 586-601.
1002 [73] Panda B, Paul SC, Mohamed NAN, Tay YWD, Tan MJ. Measurement of tensile bond strength of 3D
1003 printed geopolymer mortar, Measurement. 113 (2018) 108-16.
1004 [74] Al-Qutaifi S, Nazari A, Bagheri A. Mechanical properties of layered geopolymer structures applicable
1005 in concrete 3D-printing, Constr Build Mater. 176 (2018) 690-9.
1006 [75] Van Der Putten J, De Schutter G, Van Tittelboom K. The Effect of Print Parameters on the
1007 (Micro)structure of 3D Printed Cementitious Materials. In: T Wangler, RJ Flatteditors. Cham: Springer
1008 International Publishing, 2019. 234-44.
1009 [76] Moini M, Olek J, Magee B, Zavattieri P, Youngblood J. Additive Manufacturing and Characterization
1010 of Architectured Cement-Based Materials via X-ray Micro-computed Tomography. In: Editor, T Wangler,
1011 RJ Flatteditors. RILEM Bookseries2019. 176-89.
1012 [77] Panda B, Noor Mohamed NA, Tay YWD, Tan MJ. Bond Strength in 3D Printed Geopolymer Mortar.
1013 In: T Wangler, RJ Flatteditors. Cham: Springer International Publishing, 2019. 200-6.
1014 [78] Panda B, Noor Mohamed NA, Paul SC, Bhagath Singh G, Tan MJ, Šavija B. The Effect of Material
1015 Fresh Properties and Process Parameters on Buildability and Interlayer Adhesion of 3D Printed Concrete,
1016 Materials. 12(13) (2019) 2149.
1017 [79] Wolfs RJM, Bos FP, Salet TAM. Hardened properties of 3D printed concrete: The influence of process
1018 parameters on interlayer adhesion, Cement Concrete Res. 119 (2019) 132-40.
1019 [80] Mechtcherine V, Shyshko S. Simulating the behaviour of fresh concrete with the Distinct Element
1020 Method – Deriving model parameters related to the yield stress, Cement and Concrete Composites. 55 (2015)
1021 81-90.
1022 [81] Duballet R, Baverel O, Dirrenberger J. Classification of building systems for concrete 3D printing,
1023 Automat Constr. 83 (2017) 247-58.
1024 [82] Sanjayan JG, Nematollahi B, Xia M, Marchment T. Effect of surface moisture on inter-layer strength
1025 of 3D printed concrete, Constr Build Mater. 172 (2018) 468-75.
1026 [83] Marchment T, Sanjayan J. Method of Enhancing Interlayer Bond Strength in 3D Concrete Printing. In:
1027 T Wangler, RJ Flatteditors. Cham: Springer International Publishing, 2019. 148-56.
1028 [84] Marchment T, Sanjayan J, Xia M. Method of enhancing interlayer bond strength in construction scale
1029 3D printing with mortar by effective bond area amplification, Mater Design. 169 (2019) 107684.
1030 [85] Hosseini E, Zakertabrizi M, Korayem AH, Xu G. A novel method to enhance the interlayer bonding of
1031 3D printing concrete: An experimental and computational investigation, Cement and Concrete Composites.
1032 99 (2019) 112-9.
1033 [86] Zareiyan B, Khoshnevis B. Effects of interlocking on interlayer adhesion and strength of structures in
1034 3D printing of concrete, Automat Constr. 83 (2017) 212-21.
1035 [87] Feng P, Meng X, Chen J, Ye L. Mechanical properties of structures 3D printed with cementitious
1036 powders, Constr Build Mater. 93 (2015) 486-97.
1037 [88] Ma G, Zhang J, Wang L, Li Z, Sun J. Mechanical characterization of 3D printed anisotropic
1038 cementitious material by the electromechanical transducer, Smart Mater Struct. 27(7) (2018) 75036.
1039 [89] Ma G, Li Z, Wang L, Bai G. Micro-cable reinforced geopolymer composite for extrusion-based 3D
1040 printing, Mater Lett. 235 (2019) 144-7.
1041 [90] Hambach M, Volkmer D. Properties of 3D-printed fiber-reinforced Portland cement paste, Cement and
1042 Concrete Composites. 79 (2017) 62-70.
1043 [91] Paul SC, Tay YWD, Panda B, Tan MJ. Fresh and hardened properties of 3D printable cementitious
1044 materials for building and construction, Arch Civ Mech Eng. 18(1) (2018) 311-9.
1045 [92] Rosa, Maria, Espinosa, And, Lutz, Franke. Influence of the age and drying process on pore structure
1046 and sorption isotherms of hardened cement paste, Cement & Concrete Research.(36) (2006) 1969-84.
1047 [93] Mehta PK, Monteiro PJM. Concrete: Microstructure, Properties and Materials. 3rd ed: McGraw-Hill
1048 Professional, 2006.

[94] Ma G, Wang L, Ju Y. State-of-the-art of 3D printing technology of cementitious material—An emerging technique for construction, Science China Technological Sciences. 61(4) (2018) 475-95.
[95] Wu L, Farzadnia N, Shi C, Zhang Z, Wang H. Autogenous shrinkage of high performance concrete: A review, Constr Build Mater. 149 (2017) 62-75.
[96] Zhutovsky S, Kovler K. Effect of internal curing on durability-related properties of high performance concrete, Cement Concrete Res. 42(1) (2012) 20-6.
[97] Papachristoforou M, Mitsopoulos V, Stefanidou M. Use of by-products for partial replacement of 3D printed concrete constituents; rheology, strength and shrinkage performance, Frattura ed Integrità Strutturale. 13(50) (2019) 526-36.
[98] Rahul AV, Santhanam M, Meena H, Ghani Z. 3D printable concrete: Mixture design and test methods, Cement and Concrete Composites. 97 (2019) 13-23.
[99] Tay YWD, Qian Y, Tan MJ. Printability region for 3D concrete printing using slump and slump flow test, Composites Part B: Engineering. 174 (2019) 106968.
[100] Zhang Y, Zhang Y, Liu G, Yang Y, Wu M, Pang B. Fresh properties of a novel 3D printing concrete ink, Constr Build Mater. 174 (2018) 263-71.
[101] Mechtcherine V, Nerella VN, Will F, Näther M, Otto J, Krause M. Large-scale digital concrete construction – CONPrint3D concept for on-site, monolithic 3D-printing, Automat Constr. 107 (2019) 102933.
[102] Panda B, Tan MJ. Rheological behavior of high volume fly ash mixtures containing micro silica for digital construction application, Mater Lett. 237 (2019) 348-51.
[103] Chen M, Li L, Zheng Y, Zhao P, Lu L, Cheng X. Rheological and mechanical properties of admixtures modified 3D printing sulphoaluminate cementitious materials, Constr Build Mater. 189 (2018) 601-11.
[104] Liu Z, Li M, Weng Y, Wong TN, Tan MJ. Mixture Design Approach to optimize the rheological properties of the material used in 3D cementitious material printing, Constr Build Mater. 198 (2019) 245-55.
[105] de Larrard F, Ferraris CF, Sedran T. Fresh concrete: A Herschel-Bulkley material, Mater Struct. 31(7) (1998) 494-8.
[106] H. A. B, J. F. H, K W. An Introduction to Rheology: Elsevier Science, 1989.
[107] Chen Y, Chaves Figueiredo S, Yalçinkaya Ç, Çopuroğlu O, Veer F, Schlangen E. The Effect of Viscosity-Modifying Admixture on the Extrudability of Limestone and Calcined Clay-Based Cementitious Material for Extrusion-Based 3D Concrete Printing, Materials. 12(9) (2019) 1374.
[108] Panda B, Unluer C, Tan MJ. Investigation of the rheology and strength of geopolymer mixtures for extrusion-based 3D printing, Cement and Concrete Composites. 94 (2018) 307-14.
[109] Ouyang J, Tan Y, Corr DJ, Shah SP. The thixotropic behavior of fresh cement asphalt emulsion paste, Constr Build Mater. 114 (2016) 906-12.
[110] Nerella VN, Beigh MAB, Fataei S, Mechtcherine V. Strain-based approach for measuring structural build-up of cement pastes in the context of digital construction, Cement Concrete Res. 115 (2019) 530-44.
[111] Qian Y, De Schutter G. Enhancing thixotropy of fresh cement pastes with nanoclay in presence of polycarboxylate ether superplasticizer (PCE), Cement Concrete Res. 111 (2018) 15-22.
[112] Kolawole JT, Combrinck R, Boshoff WP. Measuring the thixotropy of conventional concrete: The influence of viscosity modifying agent, superplasticiser and water, Constr Build Mater. 225 (2019) 853-67.
[113] Wallevik OH, Feys D, Wallevik JE, Khayat KH. Avoiding inaccurate interpretations of rheological measurements for cement-based materials, Cement Concrete Res. 78 (2015) 100-9.
[114] Haach VG, Juliani LM, Roz MRD. Ultrasonic evaluation of mechanical properties of concretes produced with high early strength cement, Constr Build Mater. 96 (2015) 1-10.
[115] Sabbağ N, Uyanık O. Prediction of reinforced concrete strength by ultrasonic velocities, J Appl Geophys. 141 (2017) 13-23.
[116] Wolfs RJM, Bos FP, Salet TAM. Correlation between destructive compression tests and non-destructive ultrasonic measurements on early age 3D printed concrete, Constr Build Mater. 181 (2018) 447-54.
[117] Zhang Y, Zhang Y, She W, Yang L, Liu G, Yang Y. Rheological and harden properties of the high-thixotropy 3D printing concrete, Constr Build Mater. 201 (2019) 278-85.
[118] Chen Y, Veer F, Copuroglu O, Schlangen E. Feasibility of Using Low CO2 Concrete Alternatives in Extrusion-Based 3D Concrete Printing. In: Editor, T Wangler, RJ Flatteditors. RILEM Bookseries2019. 269-76.

[119] Lu B, Qian Y, Li M, Weng Y, Leong KF, Tan MJ, et al. Designing spray-based 3D printable cementitious materials with fly ash cenosphere and air entraining agent, Constr Build Mater. 211 (2019) 1073-84.
[120] Chen, Li, Figueiredo C, Çopuroğlu, Veer, Schlangen. Limestone and Calcined Clay-Based Sustainable Cementitious Materials for 3D Concrete Printing: A Fundamental Study of Extrudability and Early-Age Strength Development, Applied Sciences. 9(9) (2019) 1809.
[121] Chen M, Yang L, Zheng Y, Huang Y, Li L, Zhao P, et al. Yield stress and thixotropy control of 3D-printed calcium sulfoaluminate cement composites with metakaolin related to structural build-up, Constr Build Mater. 252 (2020) 119090.
[122] Mendoza Reales OA, Duda P, Silva ECCM, Paiva MDM, Filho RDT. Nanosilica particles as structural buildup agents for 3D printing with Portland cement pastes, Constr Build Mater. 219 (2019) 91-100.
[123] Jiao D, Shi C, Yuan Q, An X, Liu Y, Li H. Effect of constituents on rheological properties of fresh concrete-A review, Cement and Concrete Composites. 83 (2017) 146-59.
[124] Ahari RS, Erdem TK, Ramyar K. Thixotropy and structural breakdown properties of self consolidating concrete containing various supplementary cementitious materials, Cement and Concrete Composites. 59 (2015) 26-37.
[125] Balapour M, Joshaghani A, Althoey F. Nano-SiO2 contribution to mechanical, durability, fresh and microstructural characteristics of concrete: A review, Constr Build Mater. 181 (2018) 27-41.
[126] Ferraris CF, Obla KH, Hill R. The influence of mineral admixtures on the rheology of cement paste and concrete, Cement Concrete Res. 31(2) (2001) 245-55.
[127] Hou S, Duan Z, Ma Z, Singh A. Improvement on the properties of waste glass mortar with nanomaterials, Constr Build Mater. 254 (2020) 118973.
[128] Li G, Wu X. Influence of fly ash and its mean particle size on certain engineering properties of cement composite mortars, Cement Concrete Res. 35(6) (2005) 1128-34.
[129] Norhasri MSM, Hamidah MS, Fadzil AM. Applications of using nano material in concrete: A review, Constr Build Mater. 133 (2017) 91-7.
[130] Özbay E, Erdemir M, Durmuş Hİ. Utilization and efficiency of ground granulated blast furnace slag on concrete properties – A review, Constr Build Mater. 105 (2016) 423-34.
[131] Rahman MK, Baluch MH, Malik MA. Thixotropic behavior of self compacting concrete with different mineral admixtures, Constr Build Mater. 50 (2014) 710-7.
[132] Saleh Ahari R, Kemal Erdem T, Ramyar K. Effect of various supplementary cementitious materials on rheological properties of self-consolidating concrete, Constr Build Mater. 75 (2015) 89-98.
[133] Senff L, Labrincha JA, Ferreira VM, Hotza D, Repette WL. Effect of nano-silica on rheology and fresh properties of cement pastes and mortars, Constr Build Mater. 23(7) (2009) 2487-91.
[134] Siddique R. Utilization of silica fume in concrete: Review of hardened properties, Resources, Conservation and Recycling. 55(11) (2011) 923-32.
[135] Siddique R, Klaus J. Influence of metakaolin on the properties of mortar and concrete: A review, Appl Clay Sci. 43(3-4) (2009) 392-400.
[136] Wang D, Shi C, Farzadnia N, Shi Z, Jia H. A review on effects of limestone powder on the properties of concrete, Constr Build Mater. 192 (2018) 153-66.
[137] Wang D, Shi C, Farzadnia N, Shi Z, Jia H, Ou Z. A review on use of limestone powder in cement-based materials: Mechanism, hydration and microstructures, Constr Build Mater. 181 (2018) 659-72.
[138] Xu G, Shi X. Characteristics and applications of fly ash as a sustainable construction material: A state-of-the-art review, Resources, Conservation and Recycling. 136 (2018) 95-109.
[139] Zhang P, Wan J, Wang K, Li Q. Influence of nano-SiO 2 on properties of fresh and hardened high performance concrete: A state-of-the-art review, Constr Build Mater. 148 (2017) 648-58.
[140] Marchon D, Kawashima S, Bessaies-Bey H, Mantellato S, Ng S. Hydration and rheology control of concrete for digital fabrication: Potential admixtures and cement chemistry, Cement Concrete Res. 112 (2018) 96-110.
[141] Chaves Figueiredo S, Çopuroğlu O, Schlangen E. Effect of viscosity modifier admixture on Portland cement paste hydration and microstructure, Constr Build Mater. 212 (2019) 818-40.
[142] Qian Y, De Schutter G. Enhancing thixotropy of fresh cement pastes with nanoclay in presence of polycarboxylate ether superplasticizer (PCE), Cement Concrete Res. 111 (2018) 15-22.
[143] Quanji Z, Lomboy GR, Wang K. Influence of nano-sized highly purified magnesium alumino silicate clay on thixotropic behavior of fresh cement pastes, Constr Build Mater. 69 (2014) 295-300.

[144] Khalil N, Aouad G, El Cheikh K, Rémond S. Use of calcium sulfoaluminate cements for setting control of 3D-printing mortars, Constr Build Mater. 157 (2017) 382-91.
[145] Ma S, Li W, Zhang S, Ge D, Yu J, Shen X. Influence of sodium gluconate on the performance and hydration of Portland cement, Constr Build Mater. 91 (2015) 138-44.
[146] Zhang X, He Y, Lu C, Huang Z. Effects of sodium gluconate on early hydration and mortar performance of Portland cement-calcium aluminate cement-anhydrite binder, Constr Build Mater. 157 (2017) 1065-73.
[147] Zou F, Tan H, Guo Y, Ma B, He X, Zhou Y. Effect of sodium gluconate on dispersion of polycarboxylate superplasticizer with different grafting density in side chain, J Ind Eng Chem. 55 (2017) 91-100.
[148] Laskar AI, Talukdar S. Rheological behavior of high performance concrete with mineral admixtures and their blending, Constr Build Mater. 22(12) (2008) 2345-54.
[149] Ogura H, Nerella V, Mechtcherine V. Developing and Testing of Strain-Hardening Cement-Based Composites (SHCC) in the Context of 3D-Printing, Materials. 11(8) (2018) 1375.
[150] Soltan DG, Li VC. A self-reinforced cementitious composite for building-scale 3D printing, Cement and Concrete Composites. 90 (2018) 1-13.
[151] Lim JH, Panda B, Pham Q. Improving flexural characteristics of 3D printed geopolymer composites with in-process steel cable reinforcement, Constr Build Mater. 178 (2018) 32-41.
[152] Li Z, Wang L, Ma G. Method for the Enhancement of Buildability and Bending Resistance of 3D Printable Tailing Mortar, Int J Concr Struct M. 12(1) (2018) 37.
[153] Ding T, Xiao J, Zou S, Wang Y. Hardened properties of layered 3D printed concrete with recycled sand, Cement and Concrete Composites. 113 (2020) 103724.
[154] Ding T, Xiao J, Zou S, Zhou X. Anisotropic behavior in bending of 3D printed concrete reinforced with fibers, Compos Struct. 254 (2020) 112808.
[155] Xiao J, Zou S, Yu Y, Wang Y, Ding T, Zhu Y, et al. 3D recycled mortar printing: System development, process design, material properties and on-site printing, Journal of Building Engineering. 32 (2020) 101779.
[156] Duan Z, Hou S, Xiao J, Singh A. Rheological properties of mortar containing recycled powders from construction and demolition wastes, Constr Build Mater. 237 (2020) 117622.
[157] Panda B, Paul SC, Hui LJ, Tay YWD, Tan MJ. Additive manufacturing of geopolymer for sustainable built environment, J Clean Prod. 167 (2017) 281-8.
[158] Zhang D, Wang D, Lin X, Zhang T. The study of the structure rebuilding and yield stress of 3D printing geopolymer pastes, Constr Build Mater. 184 (2018) 575-80.
[159] Bong SH, Nematollahi B, Nazari A, Xia M, Sanjayan JG. Fresh and Hardened Properties of 3D Printable Geopolymer Cured in Ambient Temperature. In: Editor, T Wangler, RJ Flatteditors. RILEM Bookseries2019. 3-11.
[160] Panda B, Singh GB, Unluer C, Tan MJ. Synthesis and characterization of one-part geopolymers for extrusion based 3D concrete printing, J Clean Prod. 220 (2019) 610-9.
[161] Nematollahi B, Xia M, Bong SH, Sanjayan J. Hardened Properties of 3D Printable 'One-Part' Geopolymer for Construction Applications. In: Editor, T Wangler, RJ Flatteditors. RILEM Bookseries2019. 190-9.
[162] Malaeb Z, Hachem H, Tourbah A, Maalouf T, Hamzeh F. 3D Concrete Printing: Machine and Mix Design, International Journal of Civil Engineering & Technology. 6(6) (2015) 14-22.
[163] Ivanova I, Mechtcherine V. Effects of Volume Fraction and Surface Area of Aggregates on the Static Yield Stress and Structural Build-Up of Fresh Concrete, Materials (Basel, Switzerland). 13(7) (2020) 1551.
[164] Weng Y, Li M, Tan MJ, Qian S. Design 3D printing cementitious materials via Fuller Thompson theory and Marson-Percy model, Constr Build Mater. 163 (2018) 600-10.
[165] Lu B, Weng Y, Li M, Qian Y, Leong KF, Tan MJ, et al. A systematical review of 3D printable cementitious materials, Constr Build Mater. 207 (2019) 477-90.
[166] Shi C, Wu Z, Lv K, Wu L. A review on mixture design methods for self-compacting concrete, Constr Build Mater. 84 (2015) 387-98.